SEDIMENTOLOGY the journal of the International Association of Sedimentologists

Sedimentology (2023) **70**, 1251–1280 doi: 10.1111/sed.13078

Inside a sediment-stressed Middle Devonian carpet reef: Cave exposes details of three-dimensional facies architecture and palaeoecology

TANJA UNGER* , MATTHIEU SAILLOL† , MARKUS ARETZ† , STEPHEN LOKIER‡ , MATHIAS MUELLER* , VOLKER KARIUS§ and ADRIAN IMMENHAUSER*,¶

**Sediment and Isotope Geology, Faculty for Geosciences, Ruhr-University Bochum, Universitaetsstraße 150, 44801 Bochum, Germany (E-mail: tanja.unger@ruhr-uni-bochum.de)*

†GET – Geosciences Environment Toulouse, Université Paul Sabatier, 14 avenue Edourd Belin, 31400 Toulouse, France

‡School of Built and Natural Environment, University of Derby, Kedleston Road, Derby, DE22 1GU, UK

§Department of Sedimentology and Environmental Geology, Geoscience Center, University of Göttingen, 37077 Göttingen, Germany

¶Fraunhofer Research Institution for Energy Infrastructures and Geothermal Systems, IEG, Am Hochschulcampus 1, 44801 Bochum, Germany

Associate Editor – Ying Zhou

ABSTRACT

During the Middle Devonian, reef growth reached an acme, and corals and stromatoporoids colonized depositional niches commonly considered unfavourable for reefal organisms. This paper documents the detailed facies architecture and palaeoecology of a stratigraphically thin (*ca* 12 m, 'carpet reef'), lower Givetian reefal body exposed along the walls and ceilings of the labyrinthine passages in the Klutert Cave in western Germany. The cave exposures (*ca* 26 000 m^2 of rock surface) and data from short cores, neighbouring caves and outcrops document the growth and demise of an autoparabiostrome. The reef forms part of a parasequence with a lower carbonate and an upper clastic unit, bounded by flooding surfaces. Despite the comparatively small study area (*ca* 1 km^2), the exceptional exposure quality reveals facies changes over relatively short distances both vertical and lateral. The sedimentary matrix of the reefal build-up contains between 20 to 95 wt.-% of clay and quartz of silt to sand fraction. Based on this observation, the corals and stromatoporoids thrived in murky waters and under sediment-stressed conditions. Stromatoporoids, for example, display irregular ragged flanks, a feature that is in agreement with a sediment-stressed environment. No evidence of reduced growth rates, decreased calcification rates, or lower numbers of species is found. In fact, coral diversity and density are highest within one of the two biostromal units that show peak clastic matrix values, indicating a remarkable adaptation of reef builders to sediment-stressed conditions. The initial settlement of rugose phaceloid corals took place on a mixed clastic–carbonate substrate (the basal flooding surface). Up-section, a succession of coral–stromatoporoids is present that is here described in great detail. Reef collapse occurred when much of the accommodation space was filled, and argillaceous sediments suffocated stromatoporoids and corals in a protected, low-energy environment.

Keywords Biostrome, corals, Givetian, mixed clastic–carbonate system, reef model, stromatoporoids.

INTRODUCTION

Throughout Earth's history, carbonate platforms, particularly reefs, are characterized by a diverse range of biota that evolved, flourished, adapted or, eventually, became extinct (Wood, 1999; Lipps & Stanley Jr., 2016). Regarding reef development, the Devonian period is remarkable (Kiessling & Flügel, 2002), greenhouse conditions prevailed (van Geldern *et al.*, 2006) and the eustatic sea level was high. Low-latitude shallow tropical seas hosted extensive reefal ecosystems along the transgressed continental margins (Torsvik & Cocks, 2017; Becker *et al.*, 2020). During the Middle Devonian, reef growth reached a Phanerozoic acme in terms of both latitudinal distribution and carbonate production rates (Burchette, 1981; Copper, 2002; Copper & Scotese, 2003). Prominent case examples of Middle and Upper Devonian reefs and mounds have been documented in Belgium (Boulvain, 2007; Denayer, 2019), from the Canning Basin in Western Australia (George *et al.*, 1995; Wood, 2000) and Morocco (Król *et al.*, 2018). Arguably, because of the exceptionally favourable conditions during the Devonian, reefal ecosystems entered depositional niches that would typically be considered as hostile, or at least suboptimal, for reefal organisms (Zatoń *et al.*, 2015). Examples include sediment-stressed environments (Zapalski *et al.*, 2021) characterized by high rates of clastic influx.

Many classical studies have suggested that sediment particles smother reefal organisms, stunt or kill corals and reduce illumination for photosynthesis (Rogers, 1990; Jones *et al.*, 2015; Ricardo *et al.*, 2015). Conversely, other workers have demonstrated that carbonate-producing organisms may survive, grow and even thrive under clastic sediment influx conditions in a range of depositional settings (Woolfe & Larcombe, 1999; Wilson & Lokier, 2002; Lokier *et al.*, 2009; Zapalski *et al.*, 2021). Most previous case studies of sediment-stressed ecosystems have focused on Mesozoic and Cenozoic reefal biota, while Palaeozoic sediment–biota interaction has remained less well-understood. Moreover, despite the abundance of Devonian reefs, fossil-preservation issues, particularly where extensive dolomitization has taken place, have commonly obliterated reefal fabrics thereby limiting studies of faunal assemblages and reef constructor evolution (Wood, 1998). Often, framework organisms are preserved *ex situ* (Król *et al.*, 2018), rendering their study difficult. Where data are available, they frequently relate to Frasnian reefs (for example, Canning Basin; Wood, 1998).

This study provides a detailed facies and palaeoecological analysis of a thin (*ca* 12 metres), short lived, lower Givetian (*hemiansatus* to lower *varcus* Zone) carpet reef (in the terminology applied here) biostrome exposed as incrops in the passages of the Klutert Cave at Ennepetal (western Germany, Fig. 1A). Here, the informal term 'incrops' is used to distinguish exposures in a cave from such cropping out at Earth's surface (outcrops). High resolution three-dimensional access to the internal architecture of the biostrome (autoparabiostrome, *sensu* Kershaw, 1994) permits analysis of reef morphology, internal structure and bioconstructor interactions, and, thus, enables understanding of spatial and temporal biotic responses to environmental change. Many of these aspects are previously poorly documented from Middle Devonian shallow marine reefal ecosystems.

The aims of this paper are four-fold: (i) To place detailed sedimentological and palaeoecological findings, as documented here, in their spatial and stratigraphic context. (ii) To assess the interaction of the main reef builders (stromatoporoids, rugose and tabulate corals) based on the exceptionally well-preserved and exposed faunal assemblage. (iii) To assess the relationship between the clastic sediment input and the development/survival of the biotic assemblage. (iv) Based on these considerations, the authors aim to present a tentative model for a Middle Devonian carpet reef in a sediment-stressed environment. This study has significance for those concerned with Devonian reefal systems and their biota in general and sheds light on strategies of reefal biota to cope with less-than-favourable environments.

GEOLOGICAL SETTING

The convergence of Laurussia and Gondwana characterizes Devonian palaeogeography, eventually culminating in the closure of the Rheic Ocean during the Carboniferous (Torsvik & Cocks, 2017). During the Givetian (387.7 to 382.7 Ma), the northern part of what today forms the Rhenish Slate Mountains was situated in a marine setting at the passive southern margin of Laurussia (Langenstrassen, 1982; Basse *et al.*, 2016; Torsvik & Cocks, 2017; Fig. 2A). The study area is located north of the Remscheid–Altena Anticline in western Germany's northern part of

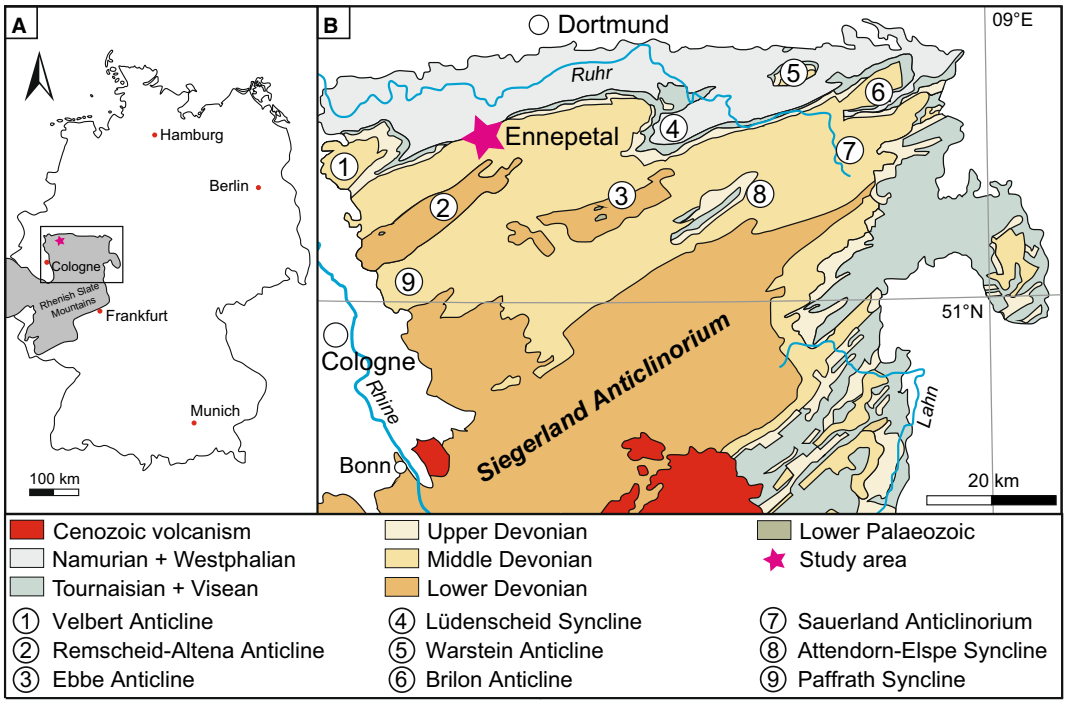

Fig. 1. (A) General map of Germany. The Rhenish Slate Mountains are located in the west. (B) Enlarged section shows the geological map of the northern Rhenish Slate Mountains. The pink star marks the study area north of the Remscheid–Altena Anticline. North of the area Middle Devonian stratigraphy is not exposed (based on Herbig, 2016; Jansen, 2019, with modifications).

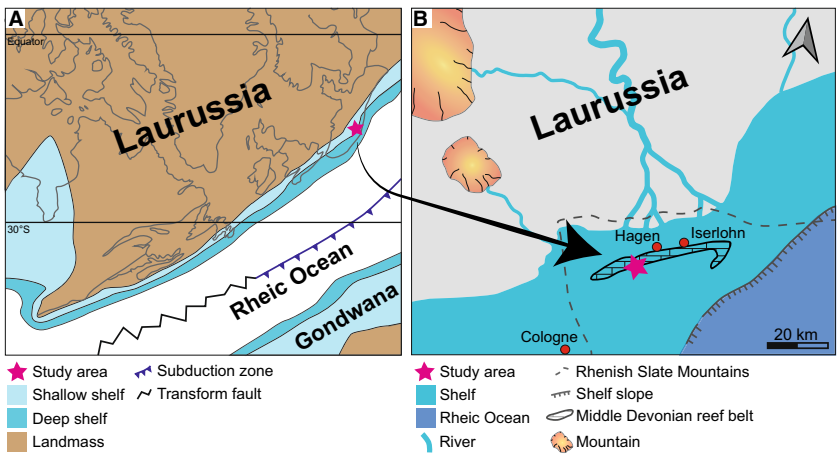

Fig. 2. (A) Middle Devonian palaeogeographical reconstruction of former Laurussia. The pink star marks the study area located on the south-western inner shelf towards the Rheic Ocean (based on Torsvik & Cocks, 2017, with modifications). (B) Schematic palaeogeographical reconstruction of the northern Rhenish Slate Mountains during lower Givetian times, with approximate position of outcrops of modern reefal limestones of the Middle Devonian. The complex studied here accounts for only a small lateral portion of the reefal system. The study area was situated south of a deltaic system (based on Langenstrassen, 1982; Meschede, 2018, with modifications).

the Rhenish Slate Mountains (Fig. 1B). In the study area, Lower Devonian shelf sedimentation was dominated by a deltaic system situated to the north, transporting clastic detritus from the Caledonian orogen (Laurussia) into the Rheic Ocean to the south (Fig. 2B; Burchette, 1981; Langenstrassen, 1983). During the Middle Devonian, a eustatic sea-level rise initiated a long-term

transgressive stage, pushing siliciclastic sediments landward and allowing for carbonate production and deposition on the shelf (Langenstrassen, 1983; May & Marks, 2013; Torsvik & Cocks, 2017). During the lower Givetian, first, albeit localized, reefal build-ups developed. Reefal diversity and distribution culminated in a regional reef-building phase of kilometre-sized structures during the upper Givetian known as the Massenkalk ('massive limestone'; May, 1991; Basse *et al.*, 2016).

The Middle Devonian strata exposed in the town of Ennepetal are assigned to the lower and upper Honsel formations, respectively (Koch, 1992). The upper Honsel formation was first described as upper Honsel beds (Denckmann, 1907). This unit comprises shales, siltstones and greywackes, that are locally interbedded with what is referred to as coral limestone (Koch, 1992). Basse *et al.* (2016) suggested that the informal term upper Honsel Formation (*sensu* Struve, 1992; May & Marks, 2013) should be avoided due to its diachronous lower stratigraphic boundary. This paper applies the informal term upper Honsel formation. The contact between the lower Honsel formation and the underlying Brandenberg unit (Fig. 3) is conformable, as is the upper Honsel formation's upper contact with the overlying Hagen–Balve Formation (Massenkalk; Fig. 3) north of Ennepetal. Overall, the upper Honsel formation records the transition from siliciclastic sedimentation (lower Honsel formation) to a reef-building phase (Massenkalk; Basse *et al.*, 2016). It is best described as shallow water deposition under fluctuating sea-level changes with turbid waters (Langenstrassen, 1983).

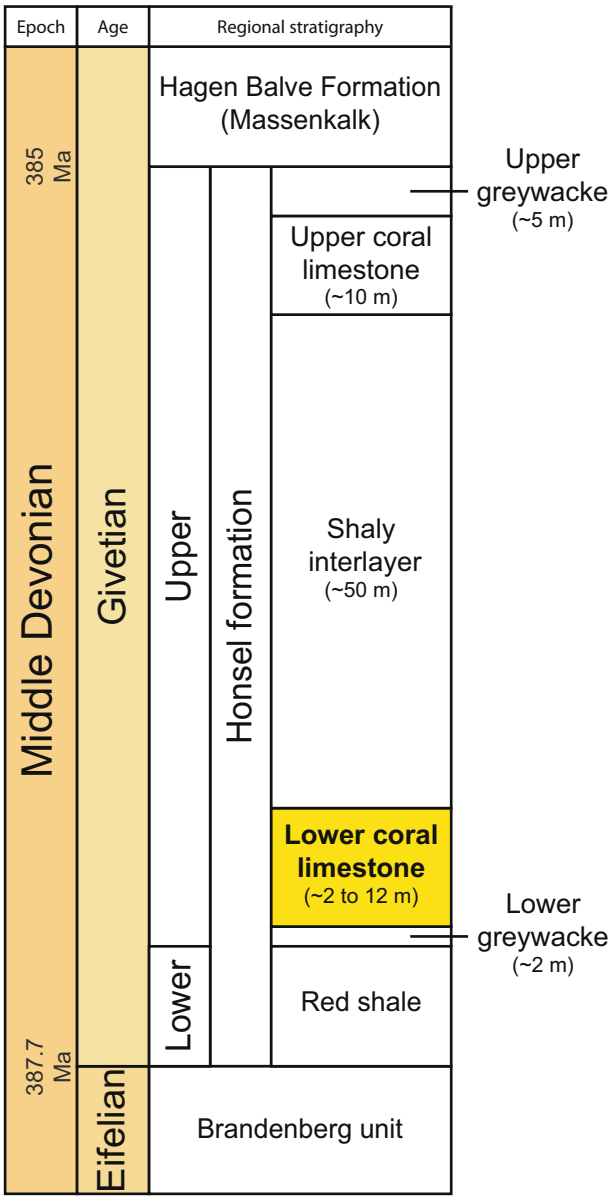

Fig. 3. Stratigraphic column of the Middle Devonian at the study area (based on Clausen & Ziegler, 1989; Koch, 1992; Cohen *et al.*, 2013; updated; Menning & Hendrich, 2016, with modifications). Lithological subdivision of the Upper Honsel formation locally defined by Koch (1992) for Ennepetal, with estimated thickness. The lower coral limestone unit represents the here studied Klutert biostrome. This interval of reef-building phase is relatively short in comparison to the overlying Massenkalk (reaching into the Frasnian, up to 1000 m in thickness; Becker *et al.*, 2016).

Klutert Cave

In the vicinity of the Klutert Cave, the upper Honsel formation dips at 10° in a north/northwest direction and is exposed in the extensive labyrinthine tunnel system of the cave that established in the lower coral limestone (Koch, 1992). The term 'Klutert biostrome' is applied throughout this paper for simplicity.

The entrance of the Klutert Cave [51°17′57″N/7°21′17″E; opens at 198 m above sea level (a.s.l.)] is located at the town of Ennepetal, Germany (Fig. 4). The first reference to the Klutert cave dates from 1686 (Clutert Höhle; Koch, 1992). With a length of 5.8 km, the Klutert Cave is the fifteenth largest cave in Germany. The age of formation of the Klutert Cave is poorly constrained. This is partially related to a lack of speleothems, thus inhibiting U-series age dating. Klutert Cave sediments (cave loam) yield spore, pollen and dinoflagellates, spanning a Cretaceous to Palaeogene/Neogene age. It seems

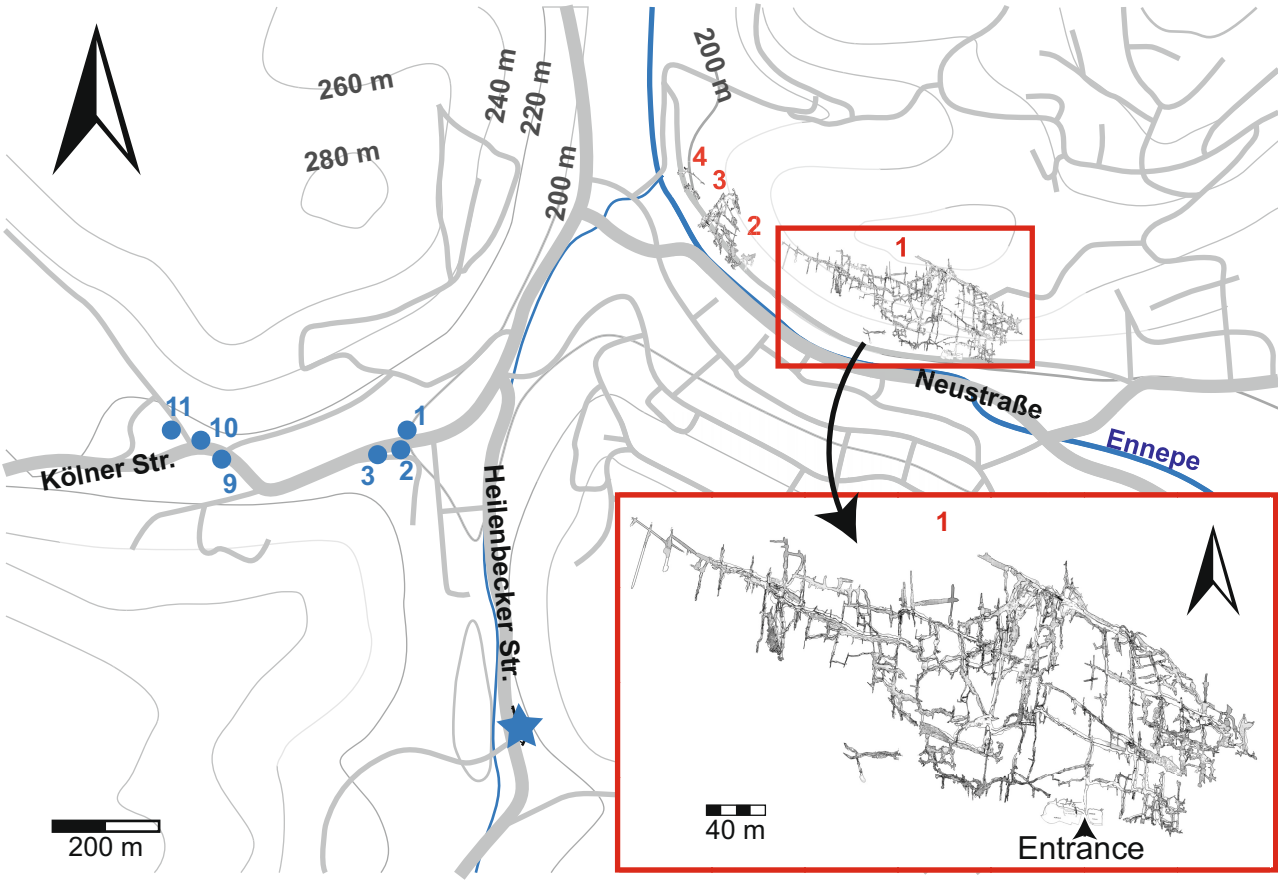

Fig. 4. Topographic map of the study area at Ennepetal. Red numbers indicate caves: (1) main study area Klutert Cave, cave map enlarged in the lower right corner (based on AKKH, 2020, with modifications); (2) Bismarck Cave; (3) Russenbunker Cave; (4) Russen Cave (based on AKKH, 2021, with modifications). Blue numbers indicate drill sites of the six short cores; blue star marks studied outcrop.

unclear whether these microfossils are: (i) erosional products of Cretaceous and younger rocks, washed into the cave at a later stage; or (ii) date the cave loams as such. Based on morphological and regional evidence, leak water corrosion or erosion as driving factors of cave development are excluded. A relation of the cave with the alluvial terraces of the Ennepe River (ages of several 100 ka) also seems unlikely, and cave development is likely older. Based on the evidence available, the Klutert Cave is best assigned as a phreatic solution cave influenced by hydrothermal activity (Koch, 1992). Unlike other caves in the region, it lacks cave decorations, and the tunnel walls are almost free of sinter. Previous work dealing with the geology and palaeontology of the Klutert Cave focused on faunal assemblages, particularly the nautiloids (Koch *et al.*, 2018a,b,c). The accessible cave passageways extend over a surface area of *ca* 500 × 200 m (Fig. 4). The recently cleaned cave walls and ceilings offer access to *ca* 26 000 m^2 of Givetian biostrome reefal facies with even minute details visible because of the excellent preservation of biota and their perfect exposure (Fig. 5).

MATERIALS AND METHODS

Fieldwork and sampling strategy

The main study site for this paper is the Klutert Cave. Additional data were collected from the Bismarck, Russen and Russenbunker caves, located 0.5 km west of Klutert Cave. Moreover, a nearby outcrop (Heilenbecker) exposes a complete section through the biostrome, albeit with moderate outcrop quality (Fig. 4). Six drill cores from a site *ca* 1.2 km south-west of the Klutert

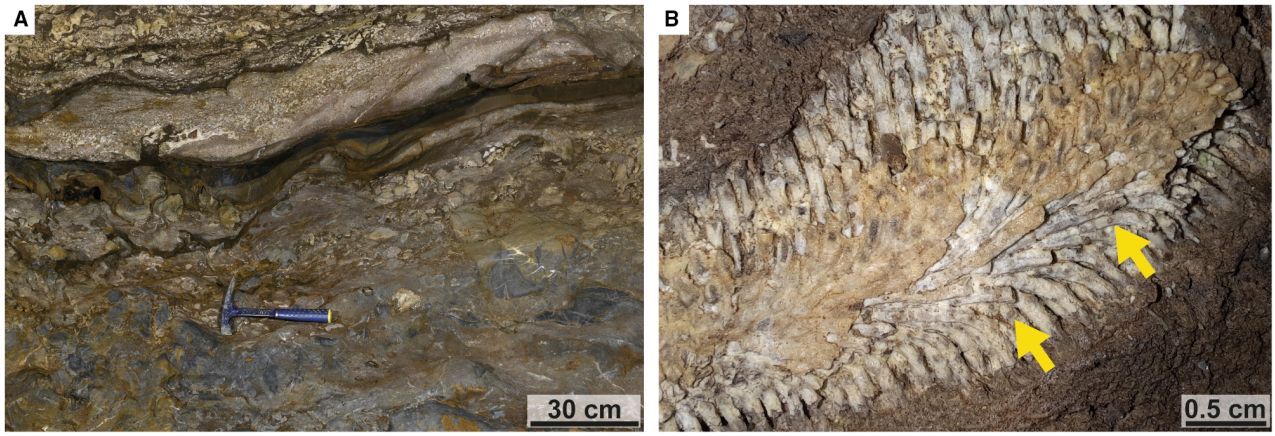

Fig. 5. (A) General view of an exemplary cave wall as an example of the preservation of the fossil biota of the Klutert biostrome. The fossils either stand out whitish from the brownish matrix or are preserved in greyish tones. Within the upper third of the image, a cavity fill of paraautochthonous thamnopores is preserved. (B) Detail picture of a tabulate coral (*Thamnopora* sp.). The extraordinary well-preserved specimens show great detail, for example pores (arrows) are macroscopically visible.

Cave (Fig. 4) were also investigated. These cores are between 4 m and 12 m in length and are referred to as cores 1, 2, 3, 9, 10 and 11, respectively. The cores cover all of the Klutert biostrome equivalents or portions thereof. The combined study sites cover a surface area of *ca* 1 km^2. Significant portions of the cave walls and ceilings were cleaned with water using a high-pressure cleaning device, with the thin clay cover and biofilm being removed. The facies associations exposed along the cave tunnel walls and ceilings were investigated using netting quadrats with a 25 × 25 cm cell size. The nets were attached to the walls, each square was photographed, and detailed facies mapping was performed.

In order to complement the information gained by the investigation of the cave walls and ceilings, a total of 45 rock samples were collected to represent the complete range of facies identified within the cave. Due to the site's protected status (the cave qualifies as a National Natural Monument), the collection of rock samples was performed without damaging the cave walls. In combination with the specimens sampled in the nearby outcrops, caves and cores, each facies type was covered by several complimentary samples.

Laboratory analyses

Microbiota and matrix carbonates were sampled for thin section and taxonomic analysis. A total of 88 thin sections from all study sites were studied using an Olympus SZ61 stereomicroscope equipped with an Olympus EP50 camera (Olympus Corporation, Tokyo, Japan). A ProScan 10 T thin section scanner provided overview scans of all thin sections (Reflecta® GmbH, Eutingen im Gäu, Germany). Facies types were described using the Embry & Klovan (1971, modified Dunham, 1962) carbonate-classification system and Dott's (1964) classification for sandstones was applied. Percentage estimations were based on charts given in Terry & Chilingar (1955). The biostrome was classified according to Kershaw (1994). Bioconstructor abundance was semi-quantitatively described as rare, present, abundant or dominant, respectively. Bioconstructor sizes are described in diameter (stromatoporoids and colonial corals; several corallites) or length (solitary rugose corals; single corallites). Bioconstructor taxonomy was performed at a level sufficient to describe lateral and stratigraphic patterns, respectively. This paper does not attempt to provide a detailed taxonomic description.

Acid digestion was performed on 38 samples collected at several study sites to establish the relative volumetric significance of siliciclastic material. Samples were selected to represent all identified facies whilst avoiding samples with an overabundance of bioclasts. Following Lokier *et al.* (2009), the samples were weighed, dissolved in HCl (10%), dried at 40°C and weighed again to measure the weight per cent (wt.-%) clastic content.

In order to obtain mineralogy data, 11 samples from the Klutert Cave were analysed utilizing

X-ray diffraction at the Georg August University Göttingen, Department of Sedimentology and Environmental Geology. Samples were crushed and later wet milled for 10 min in a McCrone mill using ethanol as fluid. Subsequently, 10 wt.-% ZnO was admixed as an internal standard and milled together with each sample. X-ray diffraction analyses were performed on an Eigenmann GmbH Orion diffractometer (XRD Eigenmann GmbH, Schnaittach-Hormersdorf, Germany), CuKα radiation 40 kV, 40 mA, primary soller slit 0.02 rad, automatic divergence slit (irradiated length 10 mm), secondary anti-scatter slit 2 mm, receiving slit 0.3 mm, Meteor E Detector. Scans were performed in the range 4° to 69.5° 2θ in steps of 0.02° 2θ, 4 s counting time per step, and in a step-scan mode. The sample diameter was 20 mm, prepared in back-loading cuvettes. Quantitative phase analyses were performed using the Rietveld software AutoQuan 2.81.

RESULTS

Klutert Cave biostrome: Facies description

Facies 1: Lower Siliciclastic Sandstone Unit

The Lower Siliciclastic Sandstone Unit forms the base of the studied section and defines the lower stratigraphic limit of the Klutert biostrome. At the main study site in the Klutert Cave, only the stratigraphically uppermost portion, *ca* 0.5 m, of this unit is exposed; hence, information is limited. The same accounts for the nearby outcrops and caves; none of the cores' sandstone portions were preserved and hence were not made accessible to the authors. Based on regional stratigraphy, the Lower Siliciclastic Sandstone facies corresponds to the uppermost part of the Lower Greywacke Unit (Fig. 6). The facies contains medium to coarse-grained, subarkosic to arkosic arenite (average grain size *ca* 0.6 mm as based on visual inspection in thin sections). This facies is dominated by quartz grains (57 to 73 wt.-%), subordinate clay minerals and feldspar (see Table S1, for details). There are rare, disarticulated, fragmented, centimetre-sized bioclasts, mainly crinoids (trochites), gastropods and unspecified shell debris, preserved within a slightly bioturbated matrix. Judging from the limited data set available, the sandstone has a partially calcareous matrix, with the carbonate content increasing from 1 wt.-% at the base of the exposed sandstones to up to 22 wt.-% at the transition to the overlying Klutert biostrome (Fig. 7A and B).

Facies 2: Coral Meadow Biostrome Unit

The Coral Meadow Biostrome (with its two subtypes) represents the initial settlement of marine reef-building organisms on a mixed clastic–carbonate substrate composed of mudstone and siltstone with bioclasts at the top of the underlying Lower Siliciclastic Sandstone Unit. The stratigraphic thickness of this unit ranges between 2 and 3 m. The term 'meadow' refers to corals colonizing one specific stratigraphic level, likely a firmground (Fig. 8A; for example, Bo *et al.*, 2009 for terminology). Branching rugose phaceloid corals (10 to 30 cm in diameter), particularly the dominant species *Disphyllum caespitosum* (Goldfuss, 1826), are exposed in an upright life position and form a bafflestone (for a detailed list of bioconstructors and their facies distribution see Table S2). Rarely, individual corals are toppled, but evidence for significant transport is lacking. Frequently, individual organisms are separated by several decimetres of sedimentary matrix rock while, in some cases, they have grown in direct contact.

The phaceloid corals' facies is referred to as Subtype A (Coral Meadow Biostrome proper). Subtype A is associated with abundant tabulate corals (5 to 10 cm in diameter), rare layered centimetre-sized stromatoporoids, solitary rugose corals (<10 cm in length), cephalopods and gastropods. Disarticulated brachiopod and millimetre-sized crinoid fragments (up to 20% based on on-site visual inspection) are present.

Subtype B (Coral Meadow and Stromatoporoid Biostrome) is dominated by branching (phaceloid) rugose corals, associated with abundant tabulate corals (depending on the species, *ca* 10 cm up to >20 cm in diameter). Moreover, layered and bulbous stromatoporoids (present to abundant; up to 10 cm in diameter), solitary rugose corals (<10 cm in length), cephalopods and gastropods are found. The matrix contains disarticulated small brachiopods and crinoids. A significant difference to subtype A of facies 2 is the occurrence of domical stromatoporoids and the abundance of solitary rugose corals and stromatoporoids.

The bioturbated host matrix of both subtypes is composed of a (micritic) mixed carbonate–clastic wackestone with 20 to 40 wt.-% siliciclastics, comprising clay minerals (associated with subordinate quartz (mainly silt size) grains). It is unclear whether or not the locally

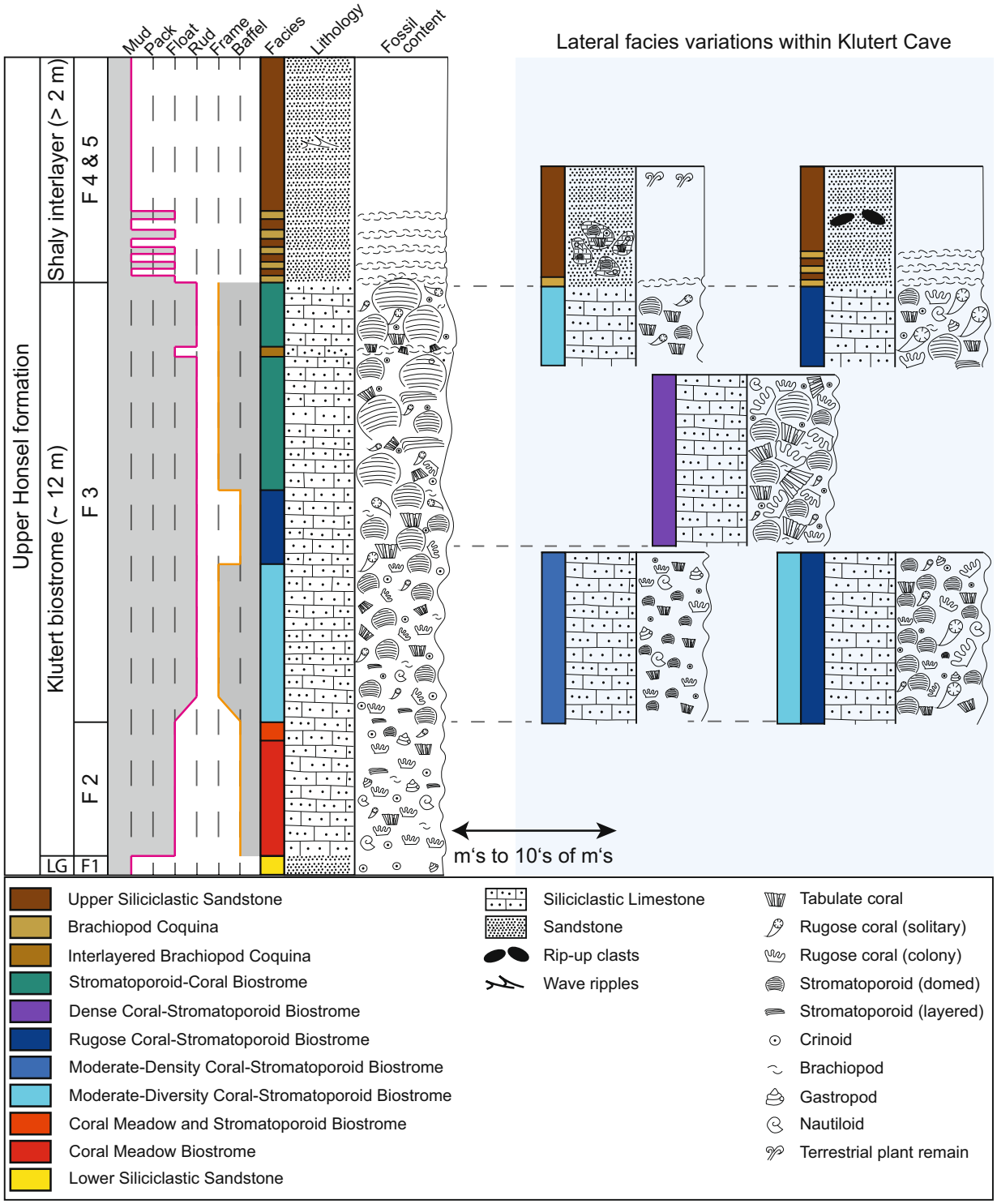

Fig. 6. Idealized composite section for the Klutert Cave. The Coral Meadow Biostrome defines the base of the Klutert biostrome, so the initial reef growth. The reefal build-up developed into the Coral Meadow and Stromatoporoid Biostrome represents the transition to the Coral–Stromatoporoid Biostrome. All subtypes of the Coral–Stromatoporoid Biostrome are arranged in a patchy way. Vertical thickness varies from decimetre to metre-scale, while horizontal distribution ranges from metre to several tens of metres. Lenses of Interlayered Brachiopod Coquina are interbedded within the Stromatoporoid–Coral Biostrome. The pink line indicates matrix and the orange line indicates bioconstructors based on the Embry & Klovan (1971, modified Dunham, 1962) classification. LG, Lower greywacke unit; Mud, Mudstone; Pack, Packstone; Float, Floatstone; Rud, Rudstone; Frame, Framestone; Baffle, Bafflestone.

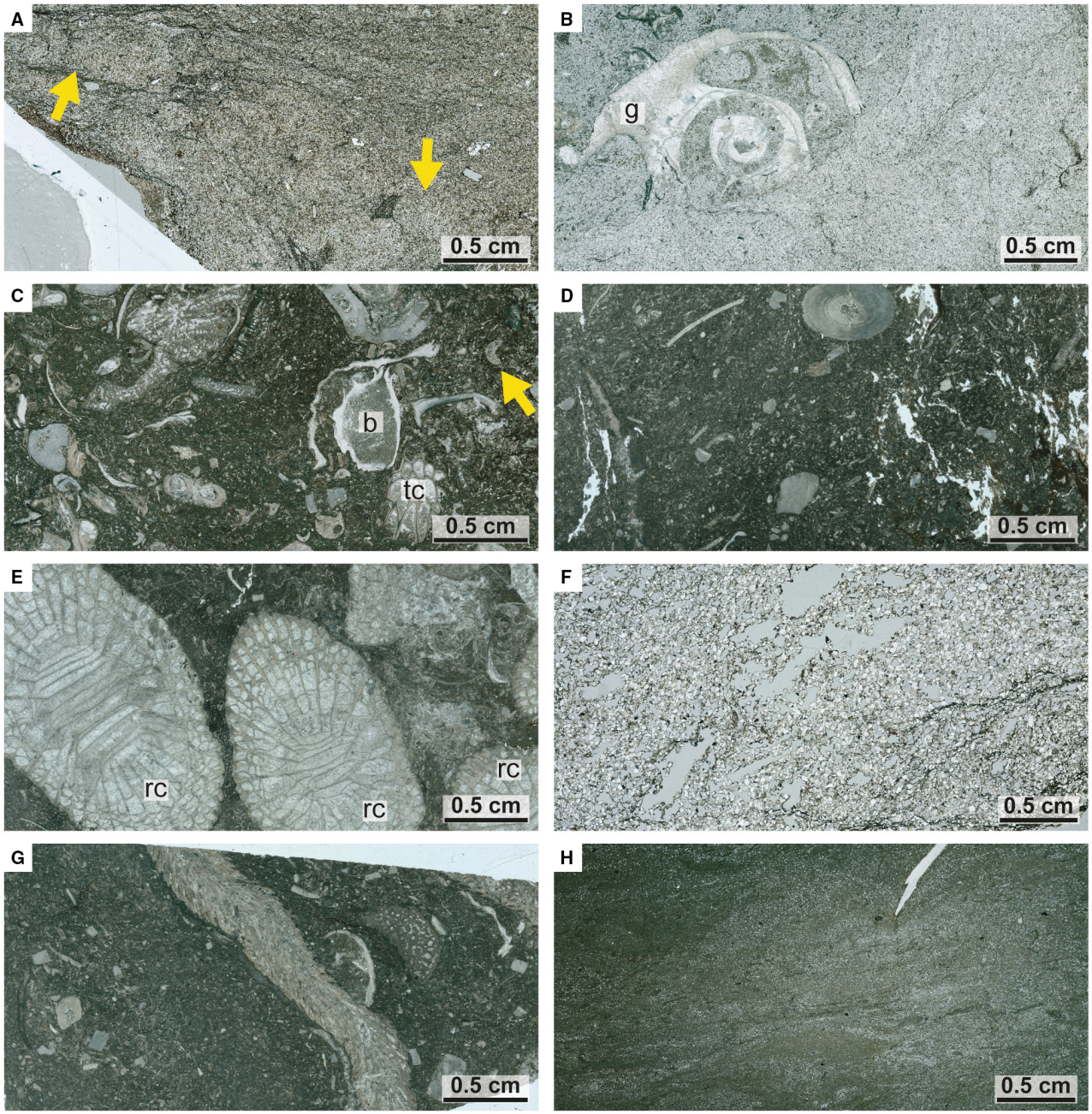

Fig. 7. Thin section photomicrographs from Klutert Cave samples. (A) The Lower Siliciclastic Sandstone shows the bioturbated (arrows) siliciclastic facies (sample KH-15-1). (B) Lower Siliciclastic Sandstone contains a fragmented gastropod (g) and reflects the up-section increase in carbonate content (sample KH-15-2). (C) Moderate-Diversity Coral–Stromatoporoid biostrome. The micritic matrix of this rudstone consists of *ca* 40 wt.-% siliciclastic content. Different bioclasts are observable, for example, brachiopod (b), tabulate coral (tc, *Thamnopora* sp.) and some crinoids (arrow) (sample KH-19). (D) Moderate-Density Coral–Stromatoporoid Biostrome. The low density of the fossil assemblage is observable macroscopically for the main reef builders and microscopically within this rudstone (sample KH-22). (E) Rugose Coral–Stromatoporoid Biostrome. Section through several phaceloid corallites of a rugose coral (rc, *Disphyllum caespitosum*) preserved within a micritic rudstone (sample KH-26). (F) and (G) Two different matrix compositions of a Dense Coral–Stromatoporoid Biostrome. (F) (sample KH-18) shows the siliciclastic-rich (>80 wt.-% siliciclastic content, quartz dominated), very coarse matrix in comparison to the carbonate-rich (<20 wt.-% siliciclastic content) matrix of (G) (sample KH-24). (H) Upper Siliciclastic Sandstone. Remarkably, the grain size is lower than within the siliciclastic-rich matrix of F3D as shown in (F) (sample KH-6).

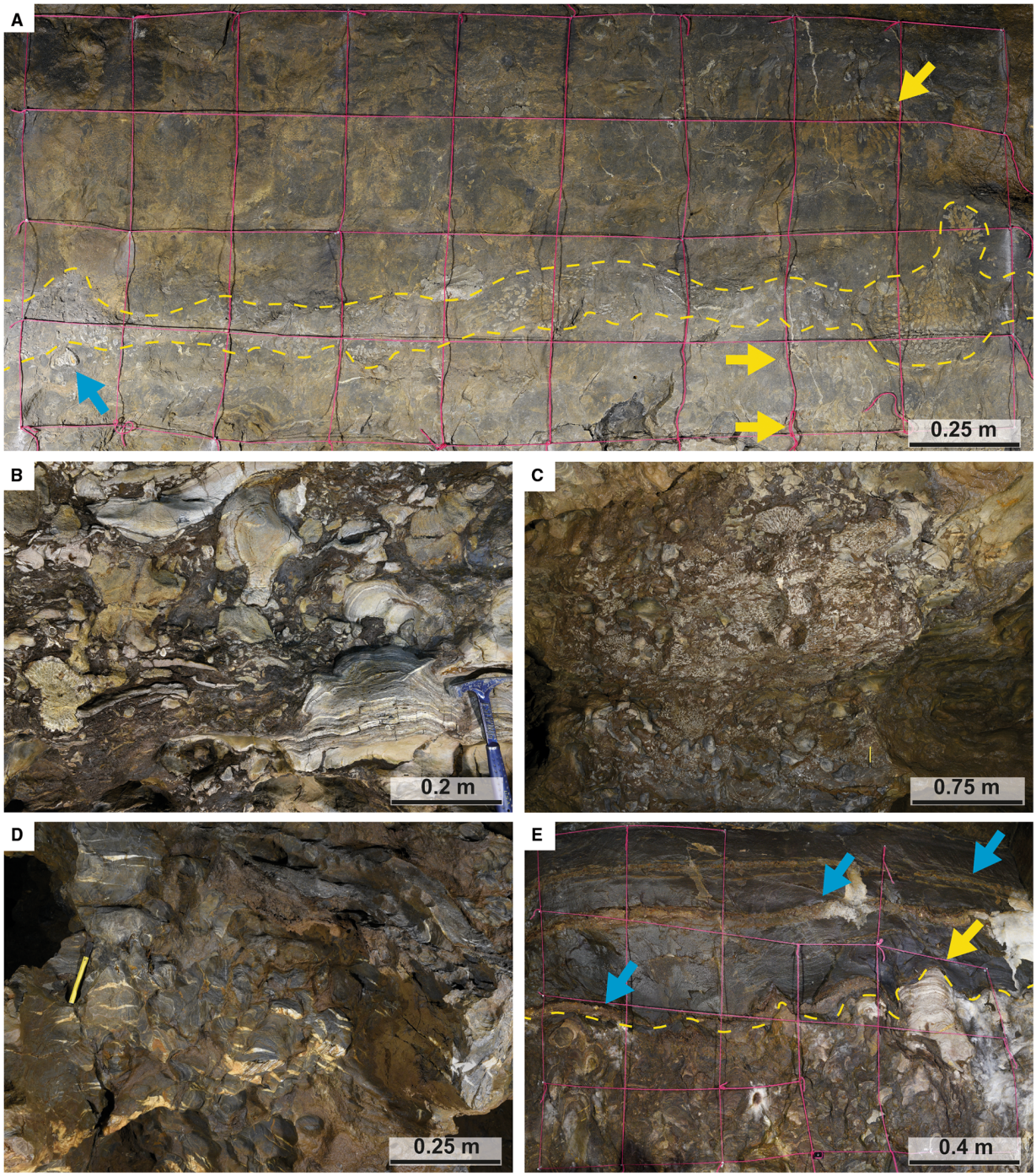

Fig. 8. (A) Portion of the cave wall representing the Coral Meadow Biostrome. Squares adjusted for detailed documentation. Yellow lines indicate one prominent layer of rugose mainly phaceloid corals (*Disphyllum caespitosum*). Further single specimens of *D. caespitosum* are preserved (yellow arrows) and one nautiloid is present (blue arrow). (B) Fossil assemblage of the Dense Coral–Stromatoporoid Biostrome. The autoparabiostrome character of this dense fabric shows relatively few interactions. (C) Fossil assemblage of the Dense Coral–Stromatopoid Biostrome. Within the siliciclastic-rich facies, frameworks of *in situ* tabulate corals such as thamnopores are preserved; typically disarticulated and paraautochthonous. (D) Fossil assemblage of the Stromatoporoid–Coral Biostrome. The whole portion of the wall comprises stromatoporoids building a dense framework. (E) Demise of the reef. The yellow line represents the reef top covered by the Brachiopod Coquina (blue arrows) and the Upper Siliciclastic Sandstone Unit. Single specimens of stromatoporoids reach into the overlying siliciclastic unit before final burying (yellow arrow).

abundant gastropods in both subtypes were hydrodynamically accumulated. Judging from the degree of preservation, however, transport distances were insignificant. At this stratigraphic level, nautiloid cephalopods, the main free-swimming biota in the studied ecosystem, reach their highest abundance.

Facies 3: Coral–Stromatoporoid Biostrome Unit

The Coral–Stromatoporoid Biostrome Unit proper (comprising five subtypes) forms the main reefal facies in the Klutert Cave. The Coral–Stromatoporoid Biostrome Unit rests conformably on the Coral Meadow Biostrome Unit. The stratigraphic thickness of this unit ranges between a minimum of 4 m (cores) and a maximum of 10 m (Klutert Cave). Three main framestone organisms are dominant: stromatoporoids, rugose and tabulate corals. Fauna associated with facies type 3 includes (dis-)articulated crinoids, brachiopods, gastropods, cephalopods, trilobites and bryozoans. Judging from direct observations in the cave and associated study site, this stratigraphic unit represents a spatially complex cluster of smaller biostromal units (each some metres to several tens of metres in diameter and some metres in height) rather than one spatially uniform unit (Fig. 6). The unit is best referred to as autoparabiostrome. Stromatoporoids are mostly preserved in life positions; tabulate and rugose corals are either autochthonous or paraautochthonous. Stromatoporoids rarely make use of coral skeletons as growth substratum. The opposite, i.e. corals encrusting stromatoporoids, is found less commonly. Bioturbation of the matrix is rarely observable. Subtypes A through to E are characteristic due to their diversity (see Table S2 for a detailed list of species distribution), abundance and size range of the different reefal organisms and their associated fauna.

Subtype A (Moderate-Diversity Coral–Stromatoporoid Biostrome) is characterized by abundant domical, bulbous and layered stromatoporoids with diameters of one decimetre to *ca* 1 m. The term diversity in the manner applied here refers to the main reef builders, particularly corals (see Table S2, for details). Stromatoporoids are associated with equally abundant rugose (predominantly solitary) corals (<10 cm in length) and locally tabulate corals (up to 20 cm in diameter). Individual corals are separated by some centimetres, rarely decimetres, of the host matrix, an argillaceous carbonate packstone (Fig. 7C) with *ca* 40 wt.-% clay to silt-sized siliciclastic material. The associated fauna includes disarticulated crinoids and brachiopods.

Subtype B (Moderate-Density Coral–Stromatoporoid Biostrome) is characterized by, in places, abundant, decimetre-sized, layered and bulbous stromatoporoids. Less commonly, mid-sized corals are present, mainly solitary rugose a few centimetres in length and tabulate corals are up to 10 cm in diameter. The spacing between individual reefal organisms is usually several centimetres, rarely corals and stromatoporoids grew so close that they touched. The associated fauna includes brachiopods, rare nautiloids and disarticulated bryozoans. The micritic matrix consists of a mixed clastic–carbonate wackestone (Fig. 7D). Occasionally, disarticulated crinoid clusters are found. The clastic content of the host matrix is in the order of 22 wt.-% and is dominated by clay minerals and silt-sized quartz grains.

The subtype C (Rugose Coral–Stromatoporoid Biostrome) is dominated by abundant corals in general, and layered and bulbous stromatoporoids ranging between one to several decimetres in diameter. On average, rugose corals are more abundant than tabulate corals. Growth morphologies define two main associations of rugose corals: One composed of phaceloid (Fig. 7E) and small (<10 cm in length) solitary corals; a second of large (>10 cm in length) solitary, often horn-shaped corals, mainly cystophylloids. Within this biostromal subunit, solitary rugose corals reach the cave's greatest dimensions (several decimetres). Conversely, tabulate corals (*Alveolites* Lamarck, 1801) remain smaller, about half the size they reach in other biostromal subunits. All of the bioconstructors build bafflestones. Based on visual inspection, disarticulated crinoids (millimetre-sized) form *ca* 30% of the matrix. Gastropods, nautiloids and brachiopods represent typical biota floating in the sedimentary matrix, albeit at highly variable abundances. Two individual trilobite pygidia were identified (*Dechenella* Kayser, 1880, and *Torleyiscutellum* Basse *et al.*, 2016.) The matrix is a mixed clastic–carbonate wackestone with 8 to 13 wt.-% clastic content dominated by clay minerals and quartz silt. The Rugose Coral–Stromatoporoid facies records the lowest clastic influx across the measured sections.

Subtype D (Dense Coral–Stromatoporoid Biostrome) is typified by a framestone growth fabric. The facies includes equal numbers of

decimetre-sized, domical stromatoporoids and corals, mainly solitary and phaceloid rugose and tabulates, at centimetre to decimetre scale. The term dense refers to individual reef builders growing in a tight fabric only separated by millimetres to centimetres of sedimentary matrix and rarely in direct contact (Fig. 8B). The rugose coral *Disphyllum quadrigeminum* (Goldfuss, 1826) displays its highest occurrence throughout the biostrome. In places, *Thamnopora* Steininger, 1831 (*in situ*) dominates across several square metres of outcrop surface (Fig. 8C). Associated fauna is represented by disarticulated crinoids, brachiopods and rarely bryozoans. The matrix comprises millimetre to centimetre-sized bioconstructor fragments in a carbonate–clastic matrix. Between 17 and 99 wt.-% of the matrix is composed of clay minerals and quartz grains. Decimetre lenses of interreef sediment, mainly sandy to silty wackestones, and locally patches of disarticulated *Thamnopora* and crinoid debris are found (Fig. 5A). Due to its spatially variable nature, the matrix qualifies as either coarse calcareous siltstone to sandstone (Fig. 7F), or micritic packstone, respectively (Fig. 7G). Throughout the sections studied, the Dense Coral–Stromatoporoid Biostrome facies is characterized by the volumetrically most significant clastic contribution. Specifically, a prominent, coarse sandstone layer (grain size 1.5 to 3.0 mm), representing a marker bed up to 40 cm thick, is correlatable across distances of *ca* 160 m within the cave.

The subtype E (Stromatoporoid–Coral Biostrome) is typified by metric, layered and domical stromatoporoids (Fig. 8D) associated with small to mid-sized solitary rugose corals. Solitary corals are 1 to 2 cm in diameter, rarely up to 5 cm; phaceloid rugose corals reach up to 20 cm in diameter. Tabulate corals (predominantly *Alveolites*) with diameters, depending on species, reach *ca* 25 cm. Individual reef builders are separated by some centimetres to a few decimetres of matrix sediment. This subtype qualified as autobiostrome in bioconstructor framestone facies. Based on visual inspection, the matrix comprises crinoids (locally up to 40–50%), scattered brachiopod valves and coral debris. The matrix rocks qualify as clastic–carbonate packstone with *ca* 89 to 95 wt.-% of a siliciclastic matrix comprising clay and quartz grains. Locally, lenses of brachiopod coquina (Interlayered Brachiopod Coquina) extend over several metres. The brachiopod coquina comprises one dominant genus (*Spinatrypa* Stainbrook, 1951) present as densely packed, (dis-)articulated shells. No other biota are found except for some disarticulated, millimetric crinoids and clusters of disarticulated *Thamnopora*. The floatstones' siliciclastic content (*ca* 28 wt.-%) is remarkably low compared to the siliciclastic-rich matrix of the Stromatoporoid–Coral Biostrome.

Facies 4: Brachiopod Coquina Unit

The Brachiopod Coquina Unit ranges in thickness between 0.5 and several centimetres and can be traced laterally over tens of metres in the Klutert Cave. Individual brachiopods are preserved as moulds, internal casts or body fossils. This facies stratigraphically overlies the reefal unit and represents the return of predominantly siliciclastic sedimentation (Fig. 6). The Upper Siliciclastic Sandstone stratigraphically overlies the Brachiopod Coquina facies. The coquina comprises densely packed (dis-)articulated brachiopod moulds and casts of one dominant genus (*Spinocyrtia* Fredericks, 1916). Locally, brachiopods are associated with disarticulated crinoids, trilobites, and rarely with corals (fragmented thamnopores and solitary rugose corals, a few centimetres in length). In some areas, centimetric clusters of trochite packstones are present. The host matrix consists of a clastic sedimentary rock that builds irregular layers, typically *ca* 3 cm thick. The contacts to the underlying and overlying facies are irregular and potentially erosive, although the reef organisms of the underlying unit show no evidence of massive erosion such as scratches or damages.

Facies 5: Upper Siliciclastic Sandstone Unit

The sandstone facies rests irregularly on the Brachiopod Coquina Unit or the Coral–Stromatoporoid Biostrome Unit and corresponds to the Shaly Interlayer Unit of the regional stratigraphy (Fig. 6). The exposed stratigraphic thickness of this unit in the Klutert Cave is 2 m or less. The siliciclastic sandstone is a bioturbated, thickly bedded, fine to coarse-grained lithic wacke with a siliciclastic content of 82 to 98 wt.-%. The sandstone comprises clay minerals, quartz grains (0.2 to 0.6 mm) and subordinate feldspar (Fig. 7H). The compositional maturity (see Table S1) of the Upper Siliciclastic Sandstone Unit is much lower than that of the sandstone facies at the base of the Klutert biostrome or of the clastic matrix of the biostrome host rock facies (F3D and E). The stratigraphically lowermost 50 cm of this unit are interbedded with up to five beds of Brachiopod Coquina (F4), as

previously described from the base of this unit (Fig. 8E). Rip-up clasts or small fragments from the underlying biostromal facies are present locally. Up-section (>1 m above the top of the Klutert biostrome), rare and disarticulated terrestrial plant remains and wave ripples are found.

Correlation and comparison of Klutert Cave biostrome to nearby study sites

Combined, the Klutert Cave and the nearby Bismarck, Russen and Russenbunker caves (Fig. 4) cover an area of *ca* 800 × 200 m. The Heilenbecker outcrop is situated at about 1 km distance, and the drill sites of the short cores considered here are within 1.1 to 1.3 km distance of the Klutert Cave. All in all, this amounts to a surface area of *ca* 1 km^2. The authors used these secondary study sites to assess the lateral continuity of observations made in the Klutert biostrome beyond the cave. Moreover, a first-order assessment of the relative proportion of clastic versus calcareous components in the sedimentary matrix was compiled across all sites (Table S3 for details).

The Russenbunker, Russen and Bismarck caves expose the stratigraphic succession that typifies the Klutert Cave, albeit with some local variability. At the entrance of the Russen Cave, the contact between the Lower Greywacke Unit and the stratigraphically lowermost units of the Klutert biostromes are exposed (Coral Meadow Biostrome). Based on acid digestion data, the sedimentary matrix of the Coral Meadow Biostrome Unit is significantly enriched in clastic material (93 wt.-%) compared to that in the Klutert Cave (42 wt.-%; Fig. 9). Phaceloid rugose corals (predominantly *Disphyllum caespitosum*) are the first and main biota colonizing the clastic sediments during the onset phase of the biostrome (see Klutert Cave Coral Meadow Biostrome). In contrast to the equivalent facies in the Klutert Cave, faunal diversity and density are lower at the Russen Cave entrance site. In the Russenbunker Cave, the contact between the Klutert biostrome and the overlying Upper Siliciclastic Sandstone Unit is exposed. Acknowledging the high level of spatial complexity in facies patterns and the regionally variable stratigraphy, this important stratigraphic level shares important attributes with the equivalent section exposed in the Klutert Cave. Examples of the facies similarity include a sandstone bed interbedded with a brachiopod coquina layer (Brachiopod Coquina Unit).

In the Bismarck Cave, coral-dominated biostromal facies is exposed. Notably, stromatoporoids are near absent. Specimens of the rugose coral *Disphyllum quadrigeminum* reach dimensions of many decimetres, making them significantly larger than their counterparts exposed in the Klutert Cave. The contact with the facies of the overlying clastic interval is similar to that exposed in the Russenbunker Cave, i.e. sandstones with one brachiopod coquina layer. Brachiopods in both caves are represented by the same dominant genus (*Spinocyrtia* sp.) as observed in the main study site, the Klutert Cave.

The Heilenbecker outcrop (Fig. 4) offers access to the full stratigraphic range of the Klutert biostrome and its overlying and underlying clastic strata, albeit at far lower outcrop quality and with less biostromal thickness (*ca* 8 m) compared to the cave incrops. Initial settlement by reefal biota is comparable in all study sites and is dominated by rugose phaceloid corals (*Disphyllum caespitosum*). Thin sections and field observations from the uppermost biostromal unit (*ca* 3 m) provide many similarities and differences with equivalent observations made at Klutert Cave. The ratio of main reef builders to associated fauna is lower than at other sites. In contrast, more trilobite fragments and bryozoans are found. In the lowermost biostromal unit, acid digestion data point to a lower clastic content in the sedimentary matrix (22 wt.-%) compared to outcrops near the Russen Cave entrance (Fig. 9).

The short drill cores offer access to minute details concerning facies and biota, albeit without lateral context. Combining information from the three-dimensional observations in the Klutert Cave with the one-dimensional core information was considered important. Facies and palaeoecology analyses are compiled, and a stratigraphic model is proposed. Figures 10 and 11 document a tentative correlation of the core facies with the overall stratigraphy of the Klutert biostrome. Within the limitations of facies correlation in a study area characterized by significant lateral and stratigraphic facies change, important similarities between the facies patterns in the Klutert Cave and the cores exist. The lowermost portions of core 1 are comparable to that characterizing the onset of reefal growth in the Klutert Cave. Similarly, the upper portions of the cores are, to some degree, comparable to the stratigraphic units that record the demise of the Klutert biostrome. It is notable that the stromatoporoid *Amphipora* sp. Schulz, 1883 is recognized in cores, yet is absent from cave incrops and the Heilenbecker outcrop.

In conclusion, the documentation of a high level of spatial and temporal facies variability over the

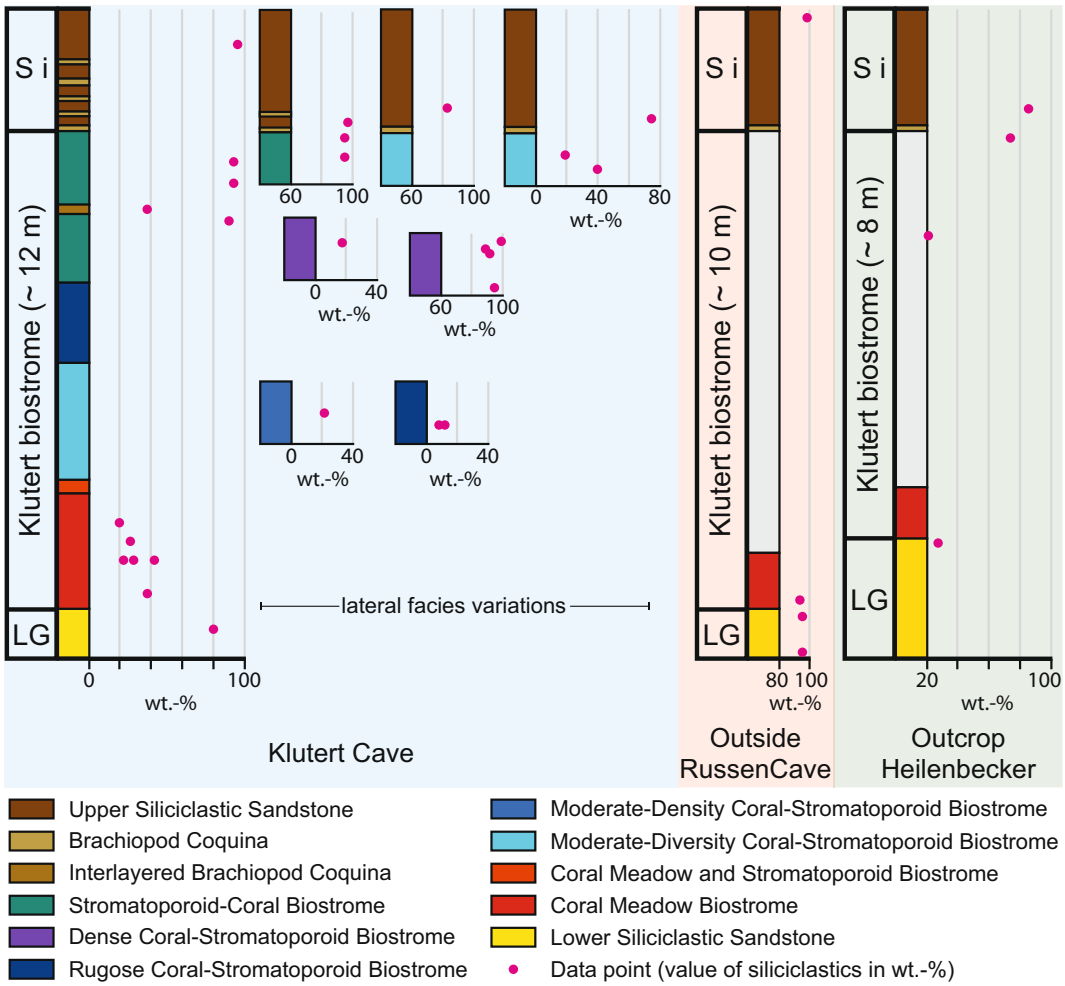

Fig. 9. Plot of the acid digestion dataset (values of siliciclastic matrix content) from the Klutert Cave, the Russen Cave natural cliff section and the outcrop Heilenbecker. All values in wt.-%. Remarkably, the siliciclastic values of the transition from the Lower Siliciclastic Sandstone Unit to the Coral Meadow Biostrome proper are much higher at the natural cliff section outside the Russen Cave than in comparison to the other study sites. The general trend of relatively high values of siliciclastics (>20 wt.-%) within the Klutert biostrome is observable in all study sites.

comparatively small surface area of *ca* 1 km^2 alone and within a stratigraphic interval less than 15 m thick is, beyond doubt, one of the important results of this study. Even when comparing the cores only (total spacing of less than 300 m), lateral facies variability is impressive (Fig. 11) and only visible due to the exceptionally detailed data set.

INTERPRETATION AND DISCUSSION

Reef habitat

Coral – Stromatoporoid dichotomy

Tightly packed reef builders and their interaction are, in essence, a prerequisite for reef framework construction and structural rigidity, for instance to withstand storm waves and current activity (see discussion in Immenhauser *et al.*, 2001). Hence, competition for space between different reef builders is a characteristic feature of reefal systems in general. With regard to Palaeozoic reefal ecosystems, the competition between corals and stromatoporoids has attracted the interest of previous research (e.g. Kershaw *et al.*, 2018, and references therein). The interaction between individual sessile reefal organisms can be classified as (i) direct competition or (ii) a live–dead association. Distinguishing these interactions in fossil reefs is challenging (Fagerstrom *et al.*, 2000). The *in situ* contact of stromatoporoids with associated

Facies Type	Subtype	Mudstone Wackestone Floatstone Other	Matrix	Main bioclasts (D: Debris/reworked ; I: *in-situ*/intact)	Secondary bioclasts (D: Debris/reworked ; I: *in-situ*/intact)	Other observations	Comparable cave facies
F1	F1a		Micrite very dark with poorly-sorted bioclasts	Brachiopods (**D**, cm)	Rugose corals (**D**); Tabulate corals *(Hillaeopora spicata)* (**D**)		F 4
	F1b			Brachiopods (**D**, mm); Rugose corals (*Acantiphyllum* sp.) (**D**)	Gastropods; Crinoids (rare)		F 3?
	F1c			*Amphipora* sp.; Brachiopods (**D**)	Rugose corals (*Acanthophylum* sp.) (**D**) Tabulate corals (**D**) (*Thamnopora* sp.; *Hillaeopora* sp.; *Favosites polymorphus*) Stromatoporoids (**D**); Gastropods	Brachiopod concentration decreases as *Amphipora*'s increases	F 3?
	F1d			Stromatoporoids (**D - I**)	Rugose corals (*Acanthophylum* sp.) (**D**) Tabulate corals (**D**) (*Thamnopora* sp.; *Hillaeopora; Favosites polymorphus*); Brachiopods (**D**)		F 3
F2	F2a		Micrite very dark with poorly-sorted bioclasts	Crinoids (**D**); Brachiopods (**D**)	Tabulate corals (**D**); Rugose corals (**D**) (rare); Gastropods		F 2/ F 3
	F2b			Stromatoporoids (**D - I**)	Brachiopods (**D**); Crinoids (**D**); Rugose (**D**) and Tabulate (**D**) corals		F 3
	F2c		Micrite with siliciclastic grains /very dark with poorly-sorted bioclasts	Crinoids (**D**); Brachiopods (**D - I**)	Rugose corals (*Cystiphyllum* sp.) (**D**); Tabulate corals *(Hillaeopora* sp.,*Favosites* sp.)(**D**) Stromatoporoids (**D - I**); Trilobites (**D**)	Brachiopods with geopetal fabrics	F 3
	F2d			Stromatoporoids (**D - I**)	Rugose corals (*Cystiphyllum* sp., *Spinophyllum* sp., *Thamnophyllum* sp.) (**D**); Tabulate corals *(Hillaeopora* sp., *Favosites sp.*) (**D**); Brachiopods (**D - I**); Crinoids (**D**)	Brachiopods with geopetal fabrics	F 3
F3	F3a		Micrite very dark with poorly-sorted bioclasts	Stromatoporoids (**D - I**)	*Amphipora* sp. (**D**); *Thamnopora* sp. (**D**); Rugose corals (**D**); Crinoids (**D**, rare); Brachiopods (**D**, rare)		F 3?
	F3b			Stromatoporoids (**D**); Rugose (**D**) (*Cystiphyllum* sp., *Acathophyllum* sp., *Heliophyllum*?, *Glosophyllum* sp., *Disphyllum*?, *Thamnophyllum*)	Tabulate corals (*Platyaxum* sp., *Alveolites* sp., *Favosites* sp., *Thamnopora* sp., *Heliolithes*?) (**D**)		F 3?
	F3c		Green matrix				
F4			Grey matrix	Stromatoporoids (**I**)	Rugose corals (*Spinophyllum* sp.) (**D**); Tabulate corals (**D**); Crinoids (**D,** rare)	Stylolites	F 3E
F5			Clastic fabric with carbonate	Brachiopods (**I**)			F 1/ F 2

Fig. 10. Tentative correlation of the core facies with the Klutert biostrome. Facies subdivision of the cores based on matrix composition, main and secondary bioclasts. Siliciclastic facies correlation is quite reasonable. Several core facies are here correlated with the Coral–Stromatoporoid Biostrome (F3), whereas a specific correlation to one of the subtypes is not possible due to scale. Cave facies: Lower Siliciclastic Sandstone Unit (F1); Coral Meadow Biostrome (F2); Coral–Stromatoporoid Biostrome (F3); Brachiopod Coquina (F4).

organisms is considered uncommon. According to Kershaw (1998), a thin sedimentary layer is usually present between the skeletal remains of individual organisms. Organisms interacting with stromatoporoids are described as epibionts and endobionts (Kershaw *et al.*, 2018). Epibionts encrust stromatoporoids and are regarded as organisms living on the stromatoporoid skeleton's surface. The host, the encrusted stromatoporoid, is considered to be dead at this time. In comparison, endobionts are described as organisms interacting with the living stromatoporoid. One example of such a live–live relationship is corals growing within a stromatoporoid accessing the growth surface with their calice (Vinn, 2016; Kershaw *et al.*, 2018).

In the Klutert Cave, the most densely packed associations of reef builders are found in the case of the Coral–Stromatoporoid Biostrome Unit (Fig. 12A). In direct contrast to the notion of two reefal organisms competing for space, the excellent incrops in the Klutert Cave reveal only a handful of cases suggesting epibiotic or endobiotic interaction between corals and stromatoporoids. Live–dead associations and live–live interactions are observed, but clear evidence that points to either of the two is not easily found. Where interaction features are present, it is mainly stromatoporoids interacting with stromatoporoids and, less commonly, corals.

The highest contact density is found in the case of the two most tightly packed facies types, the Dense Coral–Stromatoporoid Biostrome (for example, Fig. 8B) and the Stromatoporoid–Coral Biostrome. Individual organisms (primarily stromatoporoids and tabulate corals) tend to abut on or grow on top of one another (epibionts).

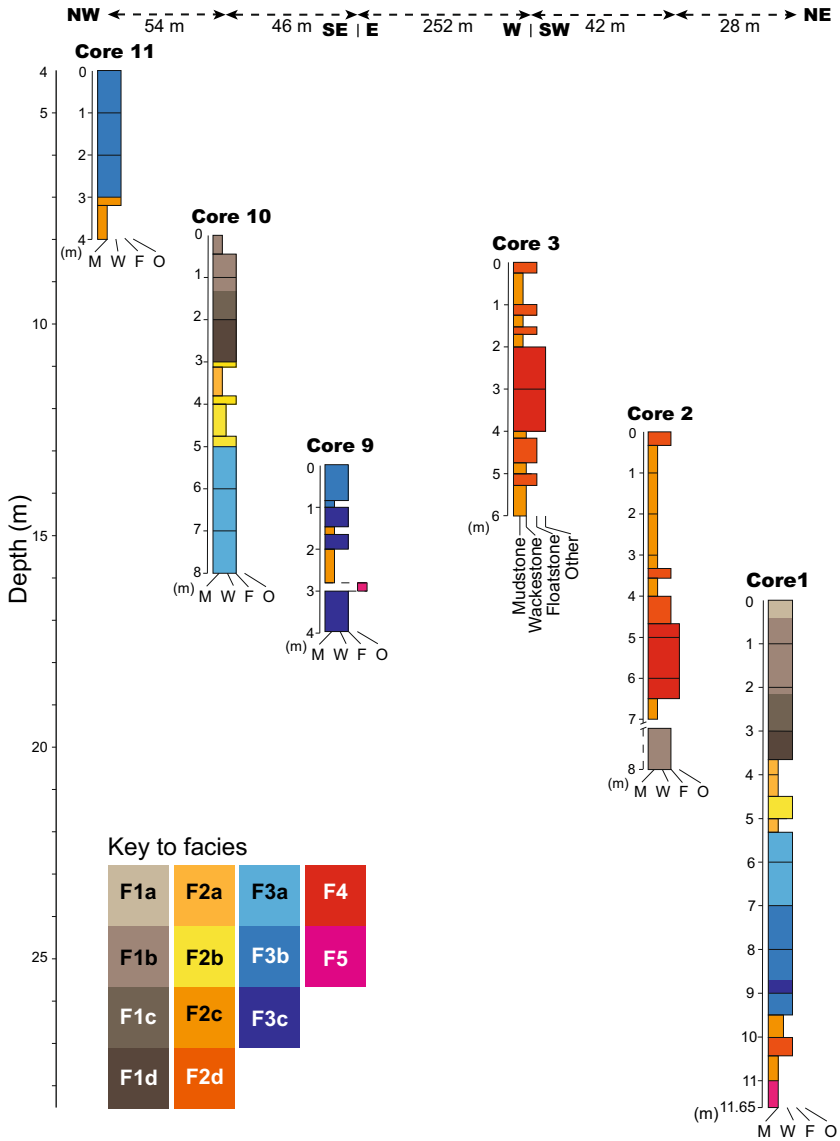

Fig. 11. Correlation of the core logs (*ca* 1.2 km south-west of Klutert Cave), relative to the exact depth (top of core 11 at 4 m below surface). Cores 11, 10 and 9 align north-west to south-east, with core 3 aligned towards the west and cores 2 and 1 aligned to the north-east. Arrangement of the core facies is similar patchy as described for the Klutert Cave. See Fig. 10 for detailed of explanation of facies F1 to F5.

Even though individual reefal organisms seem to grow in direct contact, a more detailed inspection reveals thin (millimetres to 1 cm) sediment layers that separate the two skeletons (Fig. 12B). In some cases, however, evidence for a direct growth contact is observable macroscopically and microscopically (Fig. 12C and D). Live–dead associations can be observed for stromatoporoids. Specifically, corallites of fragmented rugose coral colonies or solitary rugose corals may have been entrained by waves and currents and transported onto the growth surface of a living stromatoporoid. During further growth of the stromatoporoid animal, the coral tends to become entombed (Fig. 12E). Apparently, the overall growth of the stromatoporoids is not affected. The second type of live–dead association observed in the Klutert Cave is found in the case of the incrustation of large phaceloid rugose coral colonies by stromatoporoids (Fig. 12F). This association is restricted to coral colonies of several decimetres in width, indicating that stromatoporoid larvae selectively colonized larger coral colonies.

Endobiotic associations are observed occasionally but are less common than epibiotic interactions. Specifically, the symbiotic relationship between stromatoporoids and corals merits attention. These are commensals of a syringoporid coral within a stromatoporoid ('caunopore-association'; Fig. 12G; May, 1999). Rarely, stromatoporoids displaying evidence for this endobiotic association encrust massive tabulate corals such as favositid specimens. Within the same specimen, an endobiotic relationship can change to an epibiotic one. An example includes a syringoporid first inhabiting a stromatoporoid (Fig. 12G) and later incrusting the former (Fig. 12H). Summing up, in contrast to the preconceived notion that the exceptional exposures in the Klutert Cave would allow for the observation of numerous competing coral–stromatoporoid growth relationships, these seem to be the exception rather than the rule.

Associated fauna

Associated fauna comprises crinoids, gastropods, brachiopods, nautiloids, bryozoa and trilobites. To some degree, these provide evidence of the depositional environment relevant for this study.

Crinoids are fragmented, commonly single trochites, building up to 40 vol.-% of the matrix sediments. Rarely, fragments are presented in the form of a few attached trochites. Crinoids lived nearby or colonized reefal organisms similar to actualistic reefal settings (Clark, 1976; Messing *et al.*, 2006). Trochites described here belong to dense-fan forms that typically colonize shoreward settings of hard substrates in moderate to higher energy settings, typified by significant current activity (e.g. Holterhoff, 1997). The fact that only rarely attached trochites are found is best explained by either (punctuated) storm wave activity disintegrating and transporting crinoids or may point to the presence of significant (tidal) currents. The latter observation is perhaps not in concert with the finding of a significant clay fraction in the reefal host matrix. Alternatively, crinoids inhabited portions of the seafloor in more seaward settings – or the seafloor of inter-biostrome channel systems – and their remains were transported and deposited into the reefal setting during storms.

Gastropods are commonly accumulated in clusters within the initial Coral Meadow Biostrome. They are rarely fragmented and appear to be autochthonous to para-autochthonous in nature. Throughout the Coral–Stromatoporoid Biostrome Unit, specimens are observed but do not reach significant numbers. In sedimentary rocks associated with the carbonate-dominated Moderate-Diversity, Moderate-Density and Rugose Coral–Stromatoporoid Biostrome units, the gastropods are unfragmented. Within the siliciclastic-rich Dense Coral–Stromatoporoid Biostrome, the rare specimens are fragmented and likely transported in. Gastropods have a univalved shell, giving them a high resistance to transport damage (Flügel, 2010). Based on the number of specimens and in-life position preservation, gastropods presumably inhabited the Coral Meadow Biostrome. Specimens preserved within the biostrome unit were more likely transported in by more or less strong currents. Nowadays, gastropods inhabit a wide range of ecological niches, with the majority inhabiting shallow water (Cox, 1960). A similar relationship is inferred for the Devonian where they have been reported from various shelf environments and variable depths with the highest abundance in near-shore settings (Blodgett *et al.*, 1990). Gastropods with trochiform shells are interpreted to colonize hard substrates (Kohn, 1985), as observable within the Coral Meadow Biostrome Unit.

Brachiopods are preserved throughout all facies types as either articulated, fragmented specimens or moulds (especially Brachiopod Coquina Unit). In the Coral–Stromatoporoid Biostrome Unit, brachiopods are para-autochthonous in nature. In the Brachiopod Coquina, they are best assigned as para-autochthonous or allochthonous. Brachiopods are attached to the substratum by either a pedicle or, rarely, by cementation. Living specimens prefer hard material such as rock surfaces or corals (Rudwick, 1965). Species within the here described reefal facies are indicative of high energy settings and prefer coarse sand and silts as a substratum (Leighton, 2000). Following Langenstrassen (1983), the observed brachiopod fauna indicates a shallow depth of several metres inhabiting the proximal outer shelf. The articulated and disarticulated shells observed within the biostrome are variably-oriented and intact. This indicates a short transport of the brachiopods into the reef (Watkins, 2000), connecting the habitats.

Nautiloids are exceptionally abundant (60 out of 75 described specimens) in the Coral Meadow Unit and within the less dense facies of the biostrome (Moderate-Density and Rugose Coral–Stromatoporoid Biostrome). Therefore, it is

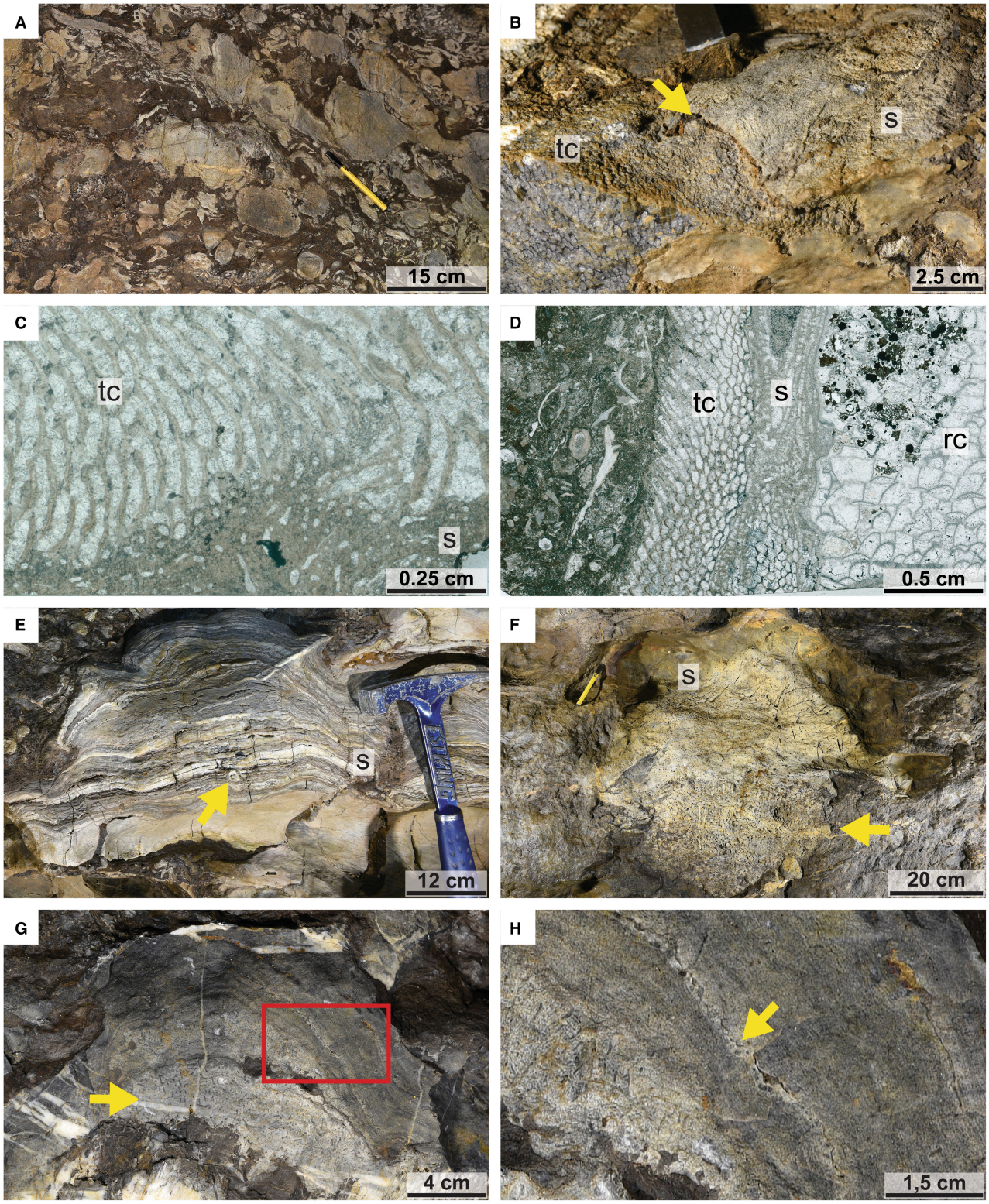

assumed that they actually lived in the habitat of the coral meadow but avoided the dense biostrome areas and have possibly been transported there. Extant nautiloids hatch in shallow waters of 100 to 200 m and migrate to deeper offshore habitats. This lifestyle is not presumed for

Fig. 12. (A) Exemplary association of the Dense Coral–Stromatoporoid Biostrome. Despite a high fossil density, single organisms are rarely in direct contact or interact with one another. (B) Interaction of two organisms. Left a tabulate coral (tc; *Favosites* sp.) growing against a stromatoporoid (s) on the right. Between the organisms, a thin sediment layer (arrow) is observable. Both organisms *in situ* with a growing direction towards the top of the image. Image provides down and side perspective. (C) Thin section photomicrograph showing live–live interaction between a tabulate coral (tc; *Alveolites* sp.) and a stromatoporoid (s). This is well-illustrated as the two organisms grew into one another (sample KH-1-1). (D) Thin section photomicrograph displaying the interaction of three organisms. On the right, a solitary rugose coral (rc) is overgrown (live–dead association) by a stromatoporoid (s), which is in live–live association with a tabulate coral (tc; *Alveolites* sp.; sample KH-9-6). (E) Stromtoporoid (s) with a rugose coral corallite (arrow) moved/transported onto the growing surface of the stromatoporoid, and subsequently encrusted by the same stromatoporoid specimen. (F) Rugose phaceloid coral (arrow; *Disphyllum caespitosum*) in decimetre-scale encrusted by a large bulbous stromatoporoid (s). (G) Live–live interaction of a syringoporid symbiont and a stromatoporoid (arrow). At a certain growth stage, the stromatoporoid stood alone, probably causing the syringoporid to encrust the stromatoporoid (enlarged view of the red box in H). (H) Live–live association of a syringoporid encrusting the stromatoporoid (arrow) that first hosted the association.

Palaeozoic ancestors with evidence from the Eifelian indicating that communities inhabited sheltered, reefal environments (Soja *et al.*, 1996).

A Givetian biostrome forming in a sediment-stressed environment

Studying ancient reef communities exposed to various stressors, such as high turbidity, low levels of light intensity, non-marine seawater salinity, low pH or critically high (or low) temperatures, has relevance for understanding modern coral communities and their possible response to environmental changes (Kleypas *et al.*, 2001; Hahn *et al.*, 2012; Santodomingo *et al.*, 2016; Zweifler *et al.*, 2021). Sediment influx and, depending on the reefal organisms, excessive sedimentation adversely affects the ecosystem's structure and function by affecting biochemical and physical processes. In modern settings and with references to scleractinian coral reefs, significant sediment input into the reefal domain is related to a reduced number of species, less live corals, lower growth rates and decreased calcification, a greater abundance of branching forms, reduced coral recruitment and slower rates of reef accretion (Rogers, 1990; Jones *et al.*, 2015). However, the presence of turbid waters or a muddy seafloor does not imply that coral growth is inhibited *per se*, and several recent studies have proposed evidence along these lines (Zweifler *et al.*, 2021). In some cases, habitats previously considered suboptimal for reef growth are now seen as important for coral diversification. This takes place by hosting a pool of species tolerant to high sediment input and low-light conditions that could occupy a wider range of habitats (Lokier *et al.*, 2009; Santodomingo *et al.*, 2016).

In the authors' view, the Givetian biostrome exposed in the study area developed within a sediment-stressed environment in a wide shelf area off the Laurussian palaeocontinent (Fig. 2B). The alternative interpretation, i.e. short and comparably rare clastic pulses (turbid water events) interrupting prolonged periods with low-sediment influx (clear waters), was not supported by the data compiled in this study. The arguments are discussed in some detail in this chapter. Based on palaeogeographical reconstructions (Fuchs, 1911; Langenstrassen, 1983; May, 1986), river systems transported clastic material onto the shelf on which these biostromes formed. This clastic material was then redistributed along the shelf by currents and waves. The resolution of palaeogeographical maps published thus far does not suffice to elaborate whether the riverine delta was separated from the open shelf biostromes by barrier islands or the like. It seems clear, however, that the Klutert biostromes grew at some distance from the river deltas, because no proximal deltaic deposits, such as conglomerates, are recorded. The notion of a fully marine depositional environment, as opposed to the typically restricted aquafacies and reduced seawater salinity near major river mouths, is confirmed by the comparably diverse marine biota, especially the stenohaline forms (crinoids and brachiopods) that accompany sessile reef builders.

Matrix analysis revealed >20 wt.-% of siliciclastic material (predominantly clay minerals and quartz grains) throughout the stratigraphic range of the biostrome interval (Fig. 9). While the silt-sized and sand-sized material may reflect punctuated influx during periods of high wave and current energy, such as storms, the significant clay fraction in the sedimentary matrix is

considered clear evidence of the persistence of turbid waters and gravitational settling. No evidence for the homogenization of specific stratigraphic levels representing punctuated clay influx events with the underlying carbonate facies is found. The fine-grained nature of the sedimentary matrix rules out constant or punctuated sediment reworking under the influence of wave orbitals. Similarly, evidence for significant sediment homogenization by means of bioturbation is lacking too. The more or less continuous influx of clastic material is also emphasized by the non-systematic vertical and lateral distribution and the variable amount of clay to sand-sized clastic material in general (Fig. 9). The stratigraphic interval typified by the Dense Coral Stromatoporoid Biostrome facies makes a good case to document this relation. Frequently, portions of this facies at one site contain 70 wt.-% more clastic material than a comparable interval less than 50 m away. This observation is in clear disagreement with the concept of homogenization of an alternating carbonate and clastic rich sedimentary matrix, but points to a complex relation of sediment transport and deposition. Compared to the stratigraphically overlying Massenkalk reef (essentially carbonates with *ca* 1 wt.-% argillaceous material), reefal organisms of the Klutert biostrome were exposed to significant clastic influx. Remarkably, the reefal biota is well-developed and shows no evidence for critically reduced calcification rates or similar. The exceptional 2D to 3D exposures in the Klutert Cave allow for detailed studies in this sense. Assuming that the above arguments hold true, it is here suggested that the Klutert biostrome offers an exceptionally suitable test case to study the response of Givetian reefal organisms to a sediment-stressed environment.

The onset of reef builder settling (rugose phaceloid corals) occurred when clastic influx temporarily decreased at the end of the deposition of the underlying Lower Siliciclastic Sandstone Unit (F1; Fig. 9). Up-section, clastic material fluctuates in terms of its volumetric significance during the growth and demise of the reef. The sedimentary matrix of the initial Coral Meadow Biostrome (F2), for example, yields between 19 to 42 wt.-% of clastic material. In a somewhat counter-intuitive manner, no difference in size or morphological properties is found regarding corals embedded in a sedimentary matrix with 20 wt.-% or with 40 wt.-% clastic material, respectively. Along similar lines, different subtypes of the Coral–Stromatoporoid Biostrome (F3) and their relative siliciclastic matrix display significant variability in clastic content (up to 95 wt.-%). None could be linked to distinct faunal changes.

The main reef builders show remarkable adaptation to their environment. This is significant because Palaeozoic corals and stromatoporoids are usually assigned to carbonate-dominated depositional environments and tolerate settings with argillaceous carbonate muds but are rarely described in combination with predominantly clastic sediments (Kershaw *et al.*, 2018). In the context of the biostrome described here, the stromatoporoid-dominated facies and the dense coral and stromatoporoid facies record a matrix with up to >85 wt.-% clastic material. The authors emphasize that there is little evidence of decreased calcification rates of the bioconstructors or other harmful effects of clastic sedimentation. Stromatoporoid growth interruptions are present in all Coral–Stromatoporoid Biostrome subtypes, regardless of the siliciclastic content of the matrix. Some specimens yield evidence for sediment layers preserved within their growth structure, while others respond to flank sedimentation through irregular growth forms (see Kershaw, 1998, for discussion).

Besides the above-described encrustation of skeletal material, the main reef builders tend to grow directly on a substratum of argillaceous carbonate. Palaeozoic corals commonly preferred soft substrates (Scrutton, 1998), whereas stromatoporoids grew on unconsolidated, partially consolidated sediments, firmgrounds or hardgrounds or skeletal debris (Kershaw *et al.*, 2018). The Klutert Cave incrops provide clear evidence that stromatoporoids colonized and grew on a predominantly soft-sediment substratum (discussion and critique in Kershaw *et al.*, 2018). Clearly, the findings presented here confirm that one of the reasons for the success of stromatoporoids is their ability to colonize fine-grained sedimentary substrates (Kershaw, 1998).

Within the Dense Coral–Stromatoporoid Biostrome, a high clastic content (>85 wt.-%) in the matrix is the rule rather than the exception. Despite the peak clastic influx, this stratigraphic interval displays the highest fossil density and coral diversity throughout the biostrome stratigraphy. Numerous other observations set this interval apart. For example, reefal organisms build a coarse framework with significant internal cavities filled by (mixed carbonate–clastic) sediment or para-autochthonous reefal debris

(Fig. 5A). None of the other stratigraphic intervals display comparably large internal cavities filled with sedimentary material. In this interval, tabulate coral (*Thamnopora* sp.) specimens are commonly preserved in life position (Fig. 8D) while in all of the other subfacies, *Thamopora* sp. are para-autochthonous. It is inferred here that the high sedimentation rate protected the organism from transport and redeposition by embedding (stabilizing) the abandoned portions of the corallum in a protective sedimentary layer. Alternatively, one may argue that the high sediment accumulation rates related to the Dense Coral–Stromatoporoid Biostrome interval point to a lower hydrodynamic level and, hence, a more protected shelf environment.

Commonly high sedimentation rates are linked to a reduced number of species and a greater abundance of branching coral forms (Rogers, 1990; Jones *et al.*, 2015). Solitary rugose cystiphylloids are the only coral species lacking from siliciclastic-rich facies, possibly due to high sedimentation rates outpacing their growth rate. Regarding the rugose corals, phaceloid corals such as *Disphyllum caespitosum* are significantly less common than cerioid forms such as *Disphyllum quadrigeminum*. Remarkably, *D. quadrigeminum* shows its highest abundance within the sediment-rich facies. In contrast, syringoporid symbionts in stromatoporoids are exclusively present in the facies that are rich in siliciclastic material (Dense Coral–Stromatoporoid Biostrome and Stromatoporoid–Coral Biostrome).

Previous work has discussed various survival strategies of reef builders exposed to high sedimentation rates. Vigorous water circulation, by means of waves and currents, sweeps fine-grained sediment from coral and stromatoporoid surfaces. Moreover, sediment accumulation and, hence, the burial of reefal organisms are prevented where the sediment is entrained and transported to deeper water settings (e.g. Woolfe & Larcombe, 1999; Wolanski *et al.*, 2005). Reefal organism morphology may also allow sediment to slip gravitationally from the biota's surface (Stafford-Smith, 1993). The extent to which active self-cleaning, as observed in recent reefs (e.g. Rogers, 1990; Stafford-Smith & Ormond, 1992; Bell, 2004), can be applied to the Palaeozoic case examples documented here is a matter of debate. However, even well-adapted organisms can only withstand a certain amount of sediment influx.

The reef's demise is documented by the final stage of mainly stromatoporoid decline on exposure to a critical level of sediment influx (Fig. 13). Based on the data obtained in the context of this study, stromatoporoids and corals declined when increasing argillaceous (clay-rich) sediment influx, affected by intrinsic or extrinsic controls, reached a critical threshold. The grain size of the sediment is particularly relevant as these reef builders had previously tolerated extended periods where significant volumes of predominantly sand-sized sediment was transported in the reefal habitat. Storm deposits, characterized by rip-up clasts and the renewed deposition of one or several Brachiopod Coquina Units, witness a distinct environmental change. Concluding, it seems likely that the reefal ecosystem was exposed to a combination of factors, each of which, when considered in isolation, was not critical but, when combined, overwhelmed the tolerance limits of the Coral–Stromatoporoid fauna.

Spatial model for a Middle Devonian carpet reef

The Klutert Cave offers access to an exceptionally well-preserved and well-exposed Coral–Stromatoporoid Biostrome. Combined with data from neighbouring study sites, these data allow a detailed spatial model to be compiled. The minute details revealed by the cave incrops shed light on the complex internal architecture of the biostrome. The question is raised of whether the sediment-stressed Klutert biostrome could serve as a template for other Devonian (or generally, Palaeozoic) sediment-stressed biostromes or if it is, in essence, an exceptional case? As a first step, a proper terminology must be established. In the sense of Riegl & Piller (1999), a coral carpet is not a proper reef (*sensu* Flügel & Kiessling, 2002). Technically speaking, the Klutert reefal complex qualifies as an autoparabiostrome (*sensu* Kershaw, 1994), indicating an evolution beyond a coral carpet stage and forming a distinct three-dimensional structure. Given the stratigraphic thickness-to-width ratio (*ca* 12 : 1000) of the Klutert biostrome, the authors apply the informal term carpet reef or biostrome to emphasize the blanket-like nature of this carbonate body.

At first glance, the architecture of the Klutert carpet reef is not directly comparable with the widely accepted Middle Devonian reef and mound models documented in the literature. Most authors define a series of sub-environments, specifically a fore-reef, a reef-core

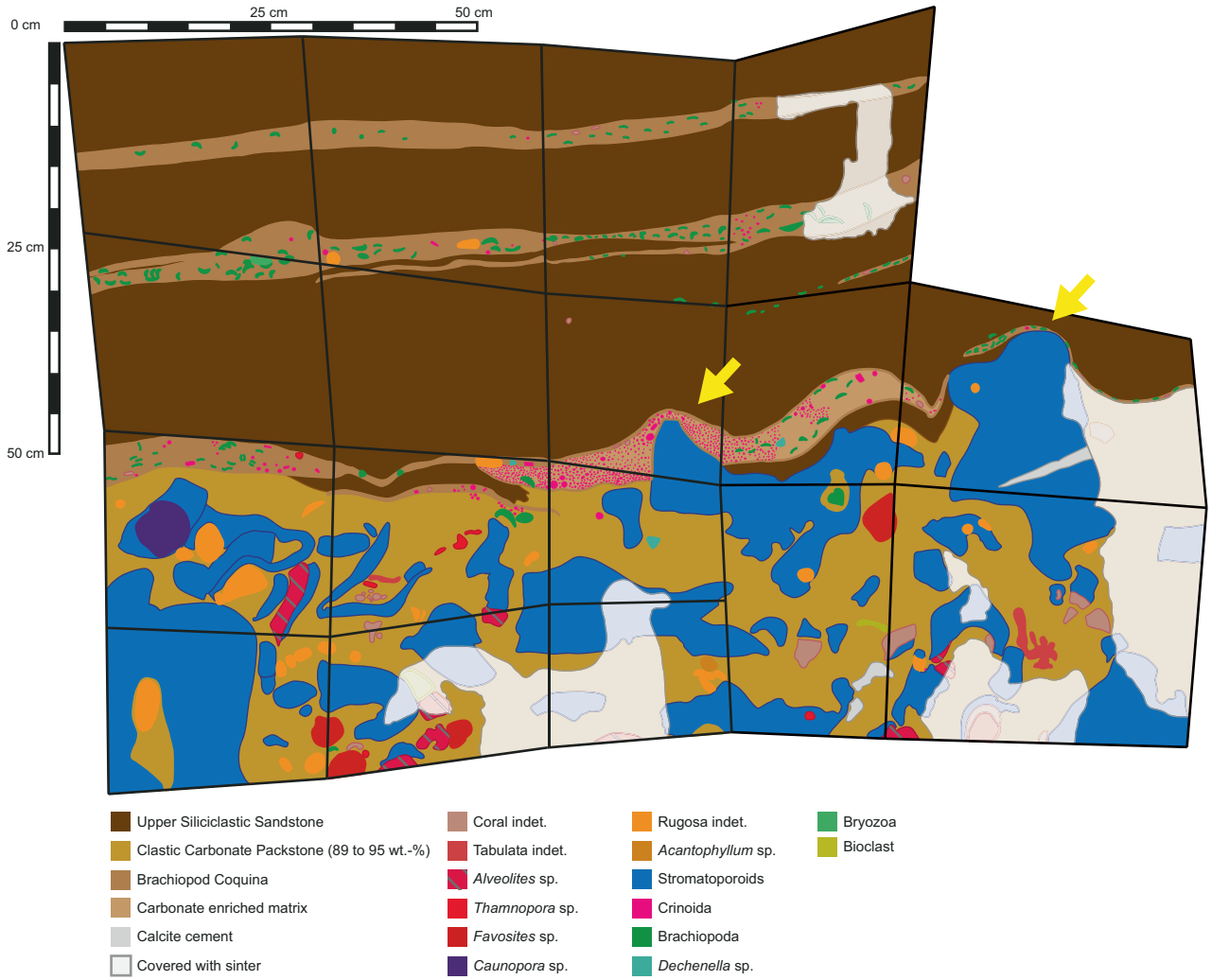

Fig. 13. Photomosaic of a portion of the cave wall, representing the demise of the reefal body (refer to Fig. 8E for overview picture; outline of the mosaic indicated by pink net in Fig. 8E). The lower half belongs to the Klutert biostrome covered by the Upper Siliciclastic Sandstone of the overlying Shaly Interlayer Unit. The struggle of the stromatoporoids to catch up with the sediment influx is well-preserved on the right half (yellow arrows).

(topographically raising above the seafloor) and a back-reef (lagoon, protected area; e.g. Machel & Hunter, 1994; Flügel, 2010). This subdivision describes an overall larger carbonate structure. Classical Devonian reef and mound structures include the Belgian case examples (Frasnian; Boulvain, 2007; Eifelian; Denayer, 2019) or the celebrated Canning Basin reefs in Western Australia (Frasnian; George *et al.*, 1995; Wood, 2000). In many cases, the stratigraphic thickness versus the lateral extent ratio of these carbonate bodies is, roughly speaking, in the order of between 100 m and 2000 m, and the regional extent is in the order of many hundreds of metres to several tens of kilometres (refer to Table 1 for an overview of classical Devonian reefs). Despite these obvious differences, the Klutert biostrome documented here shares many important similarities with other coeval reefs. The Belgian reefs, for instance, are characterized by a basal coral–crinoid association, followed by stromatoporoid-dominated facies (Lecompte, 1959; Boulvain & Vandenberghe, 2018). The Klutert biostrome displays, within the limitations of the lateral variability described here, a similar stratigraphic pattern. When comparing these reefal ecosystems (Table 1), a correlation can be established between the nature of interactions between reef builders and the corresponding sediment type and input.

The Lower Siliciclastic Sandstone Unit represents the stratigraphic base of the Klutert

Table 1. Comparison of the here studied carpet reef with a selection of Middle and Upper Devonian reefal build-ups. These were chosen to represent different Middle and Upper Devonian stages and palaeocontinents.

Name	Citation	Age	Location	Palaeo-continent	Dimensions	Diversity (coral, stromatoporoid)	Interactions	Hydro-dynamics	Sediment stressed?	Reef type/facies
Klutert Biostrome	This work	L. Givetian	N Rhenish Slate Mountains, Germany	SE shore Laurussia, NE Rheic Ocean	Lateral: >1 km^2 Thickness: 12 m	Moderate	Rare epibionts and endobionts	Moderate to high	Moderate to high	Carpet reef
Hönne Valley Reefs Complex	Becker *et al.* (2016)	Givetian to Frasnian	N Rhenish Slate Mountains, Germany	SE shore Laurussia, NE Rheic Ocean	Lateral: eastern part of *ca* 20 km long Massenkalk reef Thickness: up to 1000 m	Low to moderate	Epibionts present	Decreasing	No	Reef core and backreef facies
Strunian stromatoporoid biostromes	Herbig & Weber (1996)	'Strunian', u. Famennian	Krefeld and Aachen area, Germany	SE shore Laurussia, NE Rheic Ocean	Lateral: n.i. Thickness: 18 to 40 m	Low	Rare epibionts and endobionts	Low to moderate	Mixed carbonate siliciclastic inner ramp	Auto- to autoparabiostrome
Wellin patch reef	Denayer (2019), Król *et al.* (2021)	U. Eifelian	S Dinant Synclinorium, Belgium	SE margin Laurussia	Lateral: few hundred metres (diameter) Thickness: 100 m	Moderate to high	Common epibionts and endobionts	Low to moderate, episodically increased	Episodically increased	Patch reef
Aferdou el Mrakib	Król *et al.* (2018), Jakubowicz *et al.* (2018)	U. Eifelian to l. Givetian	SE Anti-Atlas, Morocco	Gondwana, SE Rheic Ocean	Lateral: *ca* 1 km^3 Thickness: up 130 m (estimated 200 m)	Low to moderate	Common epibionts	Low to moderate, episodically increased	Episodically increased	Reef core with forereef and backreef facies
Canning Basin	George *et al.* (1995), Wood (2000)	Givetian to Famennian	W Australia	Gondwana, approx. 15° S	Lateral: 350 × 50 km Thickness: up to 2000 m	Low to moderate	N.i.	Moderate	Episodically increased	Belt of fringing, barrier and patch reefs with backreef and forereef facies
Fanning River Reef	Zapalski *et al.* (2021)	Givetian	Queensland, Australia	E Gondwana, approx. 10° S	Lateral: 300 m Thickness: n.i.	Low (coral community)	Rare epibionts	Low, episodically increased	High	Auto- to autoparabiostrome

biostrome. This quartz-dominated, bioturbated subarkosic to arkosic arenite indicates an oxidizing seawater environment. The western part of the Klutert biostrome and, generally, the Russen Cave to the west display higher levels of clastic influx. In the case of the Dense Coral–Stromatoporoid Biostrome Unit, for example, the clastic proportion of the matrix ranges from 17 to 99 wt.-%. Within the limitations of the spatial area studied here, these patterns are indicative of an overall transport direction of clastic material from west to east. High sediment accumulation rates and elevated hydrodynamic levels prevailed. Evidence for wave and current energy comes from the fragmented and transported bioclasts. Decreasing rates of siliciclastic sedimentation, a trend from sand to silt and clay deposition and decreasing hydrodynamic levels opened a window of opportunity for the initial reefal units, specifically the Coral Meadow Biostrome Unit (Fig. 14A). Overall, environmental change is arguably linked to sea-level rise and changes in the depositional setting in the deltaic system to the north.

With the onset of the transition from the Coral Meadow Biostrome Unit to the reef-building phase proper, the Coral–Stromatoporoid Biostrome Unit, stromatoporoids grew on the coral substratum. Stromatoporoids grew larger and increased in abundance when water depths decreased (Watts, 1988; Watts & Riding, 2000). A statistically relevant increase in stromatoporoid size is a clear feature of the lower stratigraphic portions of the Klutert biostrome. If the relationship between stromatoporoid size versus water depth holds, this pattern indicates a moderate amplitude relative sea-level fall (or decreasing accommodation space, respectively).

The Klutert carpet reef is dominated by an exceptional level of internal variability over distances of some tens of metres to about 1 km (the extent of the study area). The observed variability includes the internal architecture but also east–west oriented facies patterns. Lateral facies changes are in part abrupt, and the level of complexity is so high that they cannot be explained by extrinsic factors, such as changes in energy level or water depth. In contrast, the patterns observed are typical of a system controlled by intrinsic parameters (see Walker & Alberstadt, 1975; Trensch & Strasser, 2011, for discussion), including local patterns in energy level, current velocity, seafloor topography and related sedimentation rates. Models from Burgess & Wright (2003) indicate variable regional transport, the development of sediment transport paths and mosaic of carbonate deposits to increase the complexity of reefal architecture.

The Klutert biostrome is internally organized into sub-units, specifically, some metres to several tens of metre-scale carpet reef patches that merge gradationally into the next (Figs 14B and C). This internal architecture is also present in the short cores (Fig. 11) taken at a distance of *ca* 1.2 km from the Klutert Cave and seems a general attribute of the reef studied. Possibly, initial reef growth was favoured by very localized environmental conditions, such as seafloor topography or current and wave patterns. It seems at least conceivable that these subtle differences in environmental parameters represented important threshold limits allowing reef builders to initially colonize the seafloor. It is argued that this type of internal architecture is only recognized because of the exceptional exposure conditions. The question is raised of whether other Devonian reefal bodies are organized in a similar manner? Is recognizing the metre-scale internal architecture of these carbonate bodies simply a question of outcrop conditions?

The reefal ecosystem eventually collapsed with the deposition of the Upper Siliciclastic Sandstone Unit (Fig. 14D). A limited number of stromatoporoids interfinger with the clastic unit and document the final stage of reef decline (Fig. 13). No evidence for truncation (karstification or subaquatic erosion) of the reef top is found. Brachiopod coquinas point to a protected setting and perhaps shallow water depths interrupted by punctuated high-energy events. A higher amount of clay and generally decreasing grain size compared to the matrix of the biostromal unit (western area) provide further evidence of a trend to lower hydrodynamic levels. In essence, the decrease in hydrodynamic level may be interpreted as deepening or, alternatively, as an increasingly protected environment with seaward wave–seafloor interaction resulting in low hydrodynamic levels. Wave ripples and plant remains support the notion of a seafloor at least temporarily within reach of wave orbitals (see Immenhauser, 2009, for depth range of different types of waves) and an overall coastal setting. The presence of rip-up clasts supports the notion of temporally increased hydrodynamic levels, perhaps best assigned to storm events. On the level of a working hypothesis, the authors favour the interpretation of up-section decreasing relative water depth combined with an overall low-energy

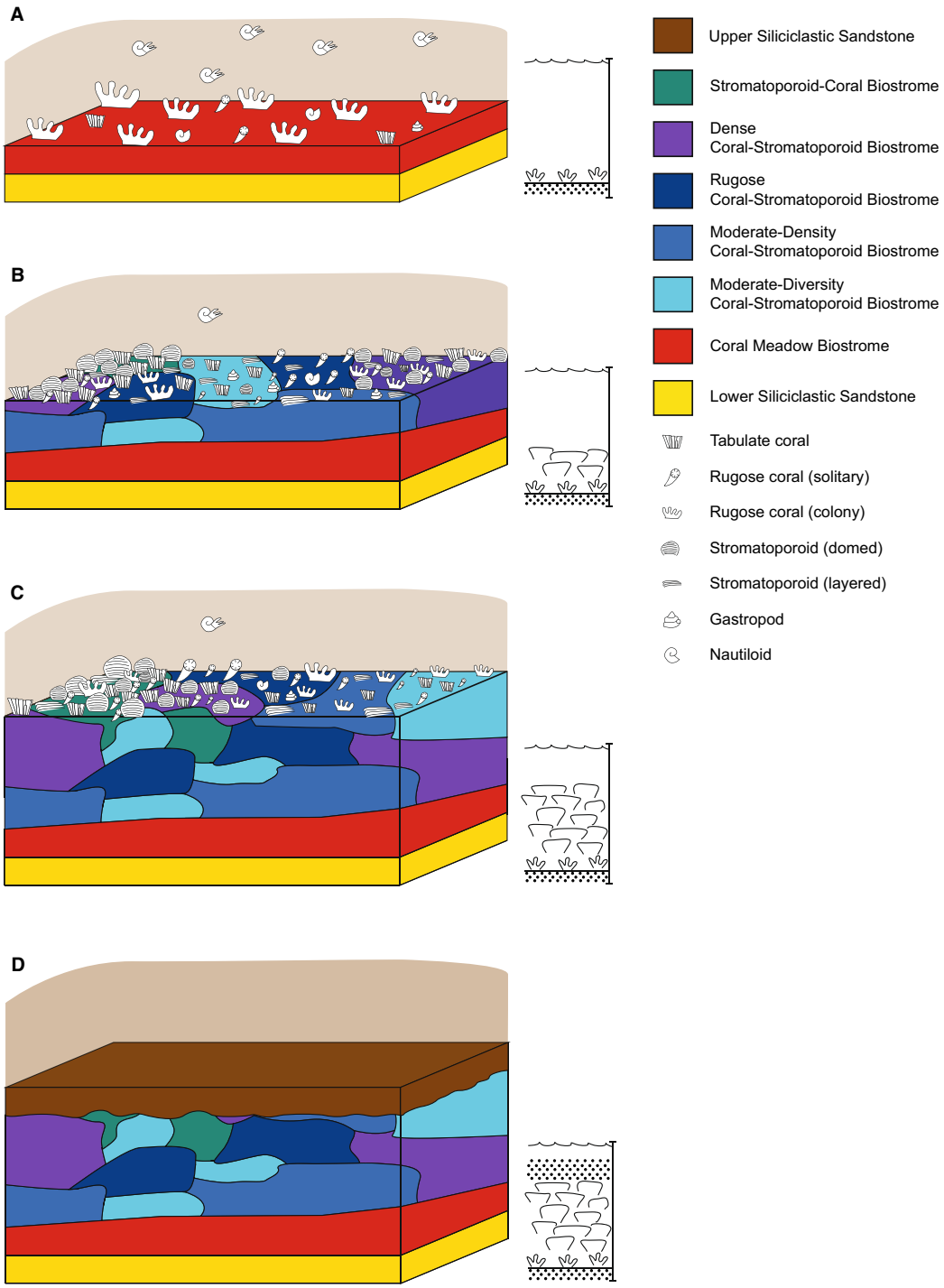

Fig. 14. (A to D) Spatial model of the here studied carpet reef, not to scale. Thickness of fully developed carpet reef is between 4 m and 12 m. (A) Initial reef settlement. During the development of the Coral Meadow Biostrome, predominantly phaceloid rugose corals settled. (B) Following the coral meadow, patches of different subunits of the Coral–Stromatoporoid Biostrome developed. Note that individual subunits are not separated by a sharp transition to a siliciclastic matrix, they rather merge gradationally into one another. (C) The arrangement of the spatially complex clusters of the subunits is observable vertically and horizontally. (D) Burial and demise of the reef system.

protected environment. Obviously, given the short time interval comprised in, and the limited stratigraphic thickness of the Klutert biostrome, comparably low-amplitude relative sea-level changes are expected. Arguably, the upward infilling of accommodation space (shoaling) was punctuated by a low-amplitude relative sea-level fall, that was insufficient to subaerially expose the reef top.

From the viewpoint of sequence stratigraphy, the Klutert biostrome and the overlying Shaly Interlayer Unit are best defined as a parasequence with a lower carbonate and an upper clastic unit (Fig. 15). The parasequence rests on a marine flooding surface, followed by a shallowing upward trend (Nichols, 2009). In general, mixed clastic–carbonate parasequences are rarely developed (Tucker, 2003) and the here described

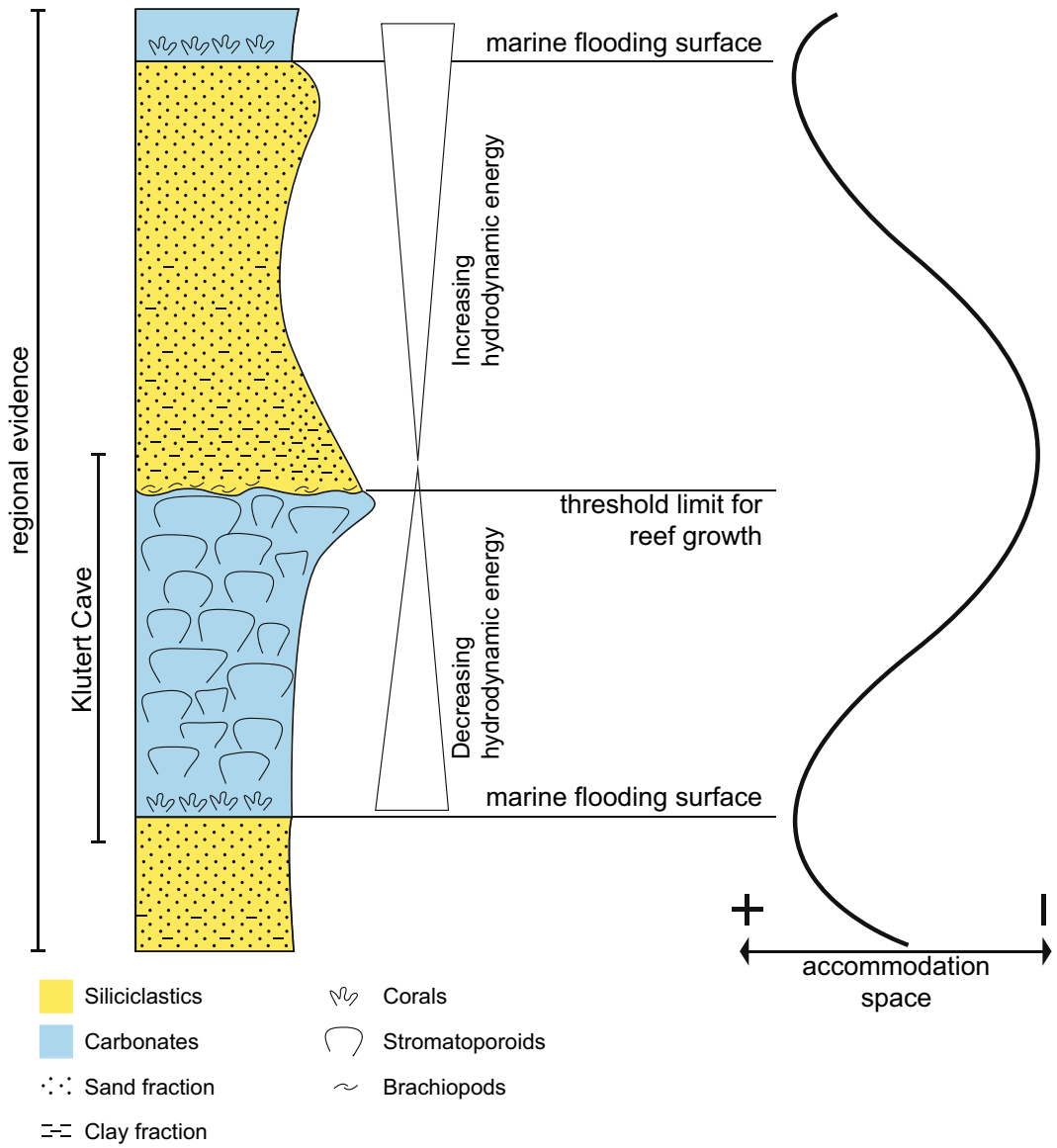

Fig. 15. Conceptual model of Klutert biostrome in the context of hydrodynamic level and accommodation space, not to scale. Thickness of carpet reef at the Klutert Cave is 12 m. In the interpretation proposed here, the Klutert biostrome and the overlying clastic unit form a parasequence bound by marine flooding surfaces at the base and top. The reef declines when the hydrodynamic level is low (most protected environment) and argillaceous sediments suffocate reef builders. Under increasing wave and current energy, argillaceous material is brought into suspension and transported away, and the threshold limit for renewed colonization by corals is reached. Reef builders show remarkable resilience to clastic influx (sand and silt fraction).

sequence is best described as *in situ* mixing (following Mount, 1984). Intrinsic variability is highly complex in mixed carbonate–siliciclastic systems (Mount, 1984; Brandano & Civitelli, 2007) and the development of a uniform sequence stratigraphic model is prohibited (Zecchin & Catuneanu, 2017). Here the initial settlement of the Coral Meadow Biostrome Unit is interpreted to represent the flooding stage (Figs 14A and 15) and the biostrome (Figs 14B, 14C and 15) that subsequently filled much of the available accommodation space. Under decreasing relative water depth and increasing clay influx, the reef collapsed, and the Upper Siliciclastic Sandstone Unit was deposited (Figs 14D and 15). The overlying marine flooding phase, with a renewed stage of initial colonization by corals (Fig. 15), is not exposed in the Klutert Cave but is recorded regionally (Koch, 1992).

CONCLUSIONS

Incrops (*ca* 26 000 m^2) in the Klutert Cave of Western Germany offer a unique opportunity to study details of the palaeoecology, facies architecture and evolution of a Middle Devonian sediment-impacted biostrome (here also labelled 'carpet reef' due to its uncommon thickness-to-width ratio; *ca* 12 : 1000). The reef was established on a shallow shelf area of the Rheic Ocean with a deltaic system situated in the north, transporting clastic detritus southward from the Caledonian orogen. The exceptional three-dimensional exposure quality, combined with nearby caves, outcrops and short cores (covering an area of *ca* 1 km^2), reveals the initiation of reef growth, its evolution and demise. The facies pattern is best explained in the sense of a parasequence with a coral carpet reflecting the initial reef stage and the marine flooding surface. Up-section, the reefal biostrome evolves, fills accommodation space and is eventually suffocated by fine argillaceous sediments that build the upper portion of the parasequence in a protected coastal environment. Throughout the evolution of the biostrome, a very significant deltaic clastic influx (>85 wt.-% continental detritus) is recorded, whereas the faunal spectrum points to normal marine seawater.

The Coral–Stromatoporoid Biostrome comprises a spatially complex cluster of smaller biostromal units. This architecture sets the Klutert biostrome apart from typical Devonian reef models, subdivided into a reef core with forereef and backreef. The Devonian reef biota (stromatoporoids, rugose and tabulate corals) display less interaction (competition, encrustation, etc.) than anticipated. Notably, the facies that reveal the highest level of clastic (sand and silt-sized quartz and clay) influx is also characterized by the highest fossil density and coral diversity. This implies that the main reef builders developed a significant level of adaptation to their environment. Based on the data compiled here, it seems likely that the reefal organisms could cope with clastic influx as long as waves and currents transported a significant proportion of the clay fraction away from the reef into deeper settings. As accommodation space decreased up-section, hydrodynamic levels also decreased, and the amount of clay deposited in the reef habitat reached a critical threshold limit.

The model presented here is relevant elsewhere because very little is known about Devonian sediment-impacted reefal systems. The exceptional outcrop quality allows for detailed observations of Givetian reef builder palaeoecology and interactions, and sheds light on the remarkable adaptation of these organisms to sediment-stressed environments. The biostrome's extremely complex and laterally variable architecture, composed of numerous patches, is remarkable given the comparably small study area of *ca* 1 km^2. The question is whether this complexity level can be recognized in less well-exposed case examples?

ACKNOWLEDGEMENTS

The authors thank the German Research Foundation (Deutsche Forschungsgemeinschaft, DFG, project: IM 44/24-1) for financial support. The authors appreciate the help of R. Bernhard, C. Fockenberg, S. Riechelmann, K. Krimmler, R. Hoffmann, N. Jöns, S. Weisel, C. Brajer, (all Ruhr-University Bochum), S. Böttcher, P. Cailly, S. Eiser, P. Heimhalt, R. Kielmann, A. Siegmund (all Klutert Cave Ennepetal), S. Voigt, S. Schild (both gem. Arbeitskreis Kluterthöhle e.V., Ennepetal) and J. Denayer (Belgium). Ages were generously provided by the Geological Survey Krefeld (conodont data) and M. Pfeil (pollen and dinoflaggelates data). An earlier version of the manuscript greatly benefited from detailed and critical comments by reviewer S. Kershaw, an anonymous colleague and Associate Editor Y. Zhou, to whom we would like to express our gratitude. Open Access funding enabled and organized by Projekt DEAL.

DATA AVAILABILITY STATEMENT

The data that supports the findings of this study are available in the supplementary material of this article.

REFERENCES

AKKH (Arbeitskreis Kluterthöhle e.V.) (2020) *Kluterthöhle Kat. Nr. 4610/006*. Arbeitskreis Kluterthöhle e.V, Ennepetal.

AKKH (Arbeitskreis Kluterthöhle e.V.) (2021) *Westlicher Bereich des Kluterthöhlensystems / Ennepetal: Bismarckhöhle Kat. Nr. 4610/004; Russenbunker Kat. Nr. 4610/009; Russenhöhle Kat. Nr. 4610/010*. Arbeitskreis Kluterthöhle e.V., Ennepetal.

Basse, M., **Koch, L.** and **Lemke, U.** (2016) *Torleyiscutellum herwigorum* n. gen., n. sp. (Trilobita) from the upper Honsel beds of the North-Western Sauerland (lower Givetian, Rhenohercynian zone), with a contribution to scutelluid systematic. *Neues Jb. Geol. Paläontol. Abh.*, **281**, 51–93.

Becker, R.T., **Aboussalam, Z.S.**, **Stichling, S.**, **May, A.** and **Eichholt, S.** (2016) The Givetian-Frasnian Hönne Valley reef complex (northern Sauerland)–an outline of stratigraphy and facies development. *Münst. Forsch. Geol. Pal.*, **108**, 126–140.

Becker, R.T., **Marshall, J.E.A.** and **Da Silva, A.-C.** (2020) The Devonian period. In: *Geologic Time Scale 2020* (Eds Gradstein, F.M., Ogg, J.G., Schmitz, M.D. and Ogg, G.M.), pp. 733–810. Elsevier, Amsterdam; Oxford; Cambridge.

Bell, J.J. (2004) Evidence for morphology-induced sediment settlement prevention on the tabular sponge *Haliclona urceolus*. *Mar. Bio.*, **146**, 29–38.

Blodgett, R.B., **Rohr, D.M.** and **Boucot, A.J.** (1990) Early and Middle Devonian gastropod biogeography. *Geol. Soc. London Mem.*, **12**, 277–284.

Bo, M., **Bavestrello, G.**, **Canese, S.**, **Giusti, M.**, **Salvati, E.**, **Angiolillo, M.** and **Greco, S.** (2009) Characteristics of a black coral meadow in the twilight zone of the Central Mediterranean Sea. *Mar. Ecol. Prog. Ser.*, **397**, 53–61.

Boulvain, F. (2007) Frasnian carbonate mounds from Belgium: sedimentology and palaeoceanography. *Geol. Soc. London Spec. Publ.*, **275**, 125–142.

Boulvain, F. and **Vandenberghe, N.** (2018) An introduction to the geology of Belgium and Luxembourg. In: *Landscapes and Landforms of Belgium and Luxembourg* (Ed. Demoulin, A.), pp. 9–33. Springer, Cham.

Brandano, M. and **Civitelli, G.** (2007) Non-seagrass meadow sedimentary facies of the Pontinian Islands, Tyrrhenian Sea: A modern example of mixed carbonate-siliciclastic sedimentation. *Sed. Geol.*, **201**, 286–301.

Burchette, T.P. (1981) European Devonian reefs: a review of current concepts and models. *SEPM Spec. Publ.*, **30**, 85–142.

Burgess, P.M. and **Wright, V.P.** (2003) Numerical forward modeling of carbonate platform dynamics: an evaluation of complexity and completeness in carbonate strata. *J. Sed. Res.*, **73**, 637–652.

Clark, A.M. (1976) Echinoderms of coral reefs. In: *Biology and Geology of Coral Reefs* (Eds Jones, O.A. and Endean, R.), pp. 95–123. Academic Press, New York, NY.

Clausen, C.-D. and **Ziegler, W.** (1989) Die neue Mittel-/Oberdevon-Grenze – ihre Anwendungsmöglichkeiten im Rheinischen Schiefergebirge. *Fortschr. Geol. Rheinl. Westfalen*, **35**, 9–30.

Cohen, K.M., **Finney, S.C.**, **Gibbard, P.L.** and **Fan, J.-X.** (2013) The ICS international chronostratigraphic chart. *Episodes*, **36**, 199–204.

Copper, P. (2002) Reef development at the Frasnian/Famennian mass extinction boundary. *Palaeogeogr. Palaeoclimatol. Palaeoecol.*, **181**, 27–65.

Copper, P. and **Scotese, C.R.** (2003) Megareefs in Middle Devonian supergreenhouse climates. *Geol. Soc. Am. Spec. Paper*, **370**, 209–230.

Cox, L.R. (1960) Gastropoda – general characteristics of Gastropoda. In: *Treatise on Invertebrate Paleontology, Part I: Molusca 1* (Ed. Moore, R.C.), pp. I84–I169. Geological Society of America and University of Kansas Press, Lawrence, KS.

Denayer, J. (2019) Revised stratigraphy of the Eifelian (Middle Devonian) of southern Belgium: sequence stratigraphy, global events, reef development and basin structuration. *Geol. Belgica*, **22**, 149–173.

Denckmann, A. (1907) Gliederung des Lennenschiefers, Blatt Hohenlimburg. *Jb. Königl. Pr. Geol. Land. Bergakad. Berlin*, **1904**, 559–565.

Dott, R.H.J. (1964) Wacke, graywacke and matrix – what approach to immature sandstone classification? *J. Sed. Petrol.*, **34**, 625–632.

Dunham, R.J. (1962) Classification of carbonate rocks according to depositional texture. In: *Classification of Carbonate Rocks. Memoir 1* (Ed. Ham, W.E.), pp. 108–121. American Association of Petroleum Geologists, Tulsa, OK.

Embry, A.F. and **Klovan, J.E.** (1971) A late Devonian reef tract on North-Eastern Banks Island, Northwest Territories. *Bull. Can. Petrol. Geol.*, **19**, 730–781.

Fagerstrom, J.A., **West, R.R.**, **Kershaw, S.** and **Cossey, P.J.** (2000) Spatial competition among clonal organisms in extant and selected Palaeozoic reef communities. *Facies*, **42**, 1–24.

Flügel, E. (2010) *Microfacies of Carbonate Rocks: Analysis, Interpretation Application*. Springer Verlag, Berlin, Heidelberg, 984 pp.

Flügel, E. and **Kiessling, W.** (2002) A new look at ancient reefs. *SEPM Spec. Publ.*, **72**, 3–10.

Fredericks, G. (1916) The palaeontological notes. 2. On some upper Palaeozoic Brachiopoda of Eurasia. *Mém. Com Géol.*, **156**, 1–88.

Fuchs, A. (1911) Blatt Iserlohn. *Erläuterungen zur Geologischen Karte von Preußen und benachbarten Bundesstaaten*, **163**, 1–63.

van Geldern, R., **Joachimski, M.M.**, **Day, J.**, **Jansen, U.**, **Alvarez, F.**, **Yolkin, E.A.** and **Ma, X.-P.** (2006) Carbon, oxygen and strontium isotope records of Devonian brachiopod shell calcite. *Palaeogeogr. Palaeoclimatol. Palaeoecol.*, **240**, 47–67.

George, A.D., **Playford, P.E.** and **Powell, C.M.** (1995) Platform-margin collapse during Famennian reef evolution, Canning Basin, Western Australia. *Geology*, **23**, 691–694.

Goldfuss, A. (1826) *Petrefacta Germaniae, Erster Theil*. Arnz & Comp., Düsseldorf, 252 pp.

Hahn, S., **Rodolfo-Metalpa, R.**, **Griesshaber, E.**, **Schmahl, W.W.**, **Buhl, D.**, **Hall-Spencer, J.M.**, **Baggini, C.**, **Fehr, K.T.** and **Immenhauser, A.** (2012) Marine bivalve shell geochemistry and ultrastructure from modern low pH environments: environmental effects versus experimental bias. *Biogeosciences*, **9**, 1897–1914.

Herbig, H.-G. (2016) Mississippian (early carboniferous) sequence stratigraphy of the Rhenish Kulm Basin, Germany. *Geol. Belgica*, **19**, 81–110.

Herbig, H.-G. and **Weber, H.M.** (1996) Facies and stromatoporoid biostromes in the Strunian (latest Devonian) of the Aachen region, Germany. *Goettinger Arb. Geol. Pal*, **2**, 359–364.

Holterhoff, P.F. (1997) Paleocommunity and evolutionary ecology of Paleozoic crinoids. *Paleontol. Soc. Pap.*, **3**, 69–106.

Immenhauser, A. (2009) Estimating palaeo-water depth from the physical rock record. *Earth Sci. Rev.*, **96**, 107–139.

Immenhauser, A., **van der Kooij, B.**, **van Vliet, A.**, **Schlager, W.** and **Scott, R.W.** (2001) An ocean-facing Aptian–Albian carbonate margin, Oman. *Sedimentology*, **48**, 1187–1207.

Jakubowicz, M., **Król, J.**, **Zapalski, M.**, **Wrzołek, T.**, **Wolniewicz, P.** and **Berkowski, B.** (2018) At the southern limits of the Devonian reef zone: Palaeoecology of the Aferdou el Mrakib reef (Givetian, eastern anti-atlas, Morocco). *Geol. J.*, **54**, 10–38.

Jansen, U. (2019) Pragian-Emsian brachiopods from the Rhenish massif (Germany): new data on evolution and biostratigraphy. *Riv. Ital. Paleontol. Stratigr.*, **125**, 735–759.

Jones, R.J., **Ricardo, G.F.** and **Negri, A.P.** (2015) Effects of sediments on the reproductive cycle of corals. *Mar. Pollut. Bull.*, **100**, 13–33.

Kayser, E. (1880) *Dechenella*, eine devonische Gruppe der Gattung Phillipsia. *Z. Deut. Geol. Ges.*, **32**, 703–707.

Kershaw, S. (1994) Classification and geological significance of biostromes. *Facies*, **31**, 81–92.

Kershaw, S. (1998) The applications of stromatoporoid palaeobiology in palaeoenvironmental analysis. *Palaeontology*, **41**, 509–544.

Kershaw, S., **Munnecke, A.** and **Jarochowska, E.** (2018) Understanding Palaeozoic stromatoporoid growth. *Earth-Sci. Rev.*, **187**, 53–76.

Kiessling, W. and **Flügel, E.** (2002) Paleoreefs – a database on phanerozoic reefs. *SEPM Spec. Publ.*, **72**, 77–92.

Kleypas, J.A., **Buddemeier, R.W.** and **Gattuso, J.-P.** (2001) The future of coral reefs in an age of global change. *Int. J. Earth Sci.*, **90**, 426–437.

Koch, L. (1992) *Das Klutert-Buch – Altes und Neues über einen der höhlenreichsten Berge Deutschlands. v.d.* Linnepe Verlag, Hagen, 316 pp.

Koch, L., **Voigt, S.** and **Brauckmann, C.** (2018a) Nautiliden aus der Kluterthöhle (Ennepetal, Nordrhein-Westfalen), aus benachbarten Höhlen und weiteren Fundorten in Oberen Honsel-Schichten (Unter-Givetium). *Geol. Pal. Westfalen*, **90**, 15–24.

Koch, L., **Voigt, S.**, **Brauckmann, C.** and **Gröning, E.** (2018b) Fossile Funde aus dem Nationalen Naturmonument Kluterthöhle (Ennepetal, Nordrhein-Westfalen). *Mitt. Verb. dt. Hoehl. Karst.*, **64**, 79–83.

Koch, L., **Voigt, S.**, **Brauckmann, C.** and **Gröning, E.** (2018c) Nautiliden-Funde aus der Kluterthöhle und der Heilenbecker Höhle (Ennepetal, Nordrhein-Westfalen) mit einem Beitrag zum Lebensraum der Nautiliden in der Korallen-Stromatoporen-Riffen der oberen Honsel-Schichten (Unter-Givetium). *Dortmunder Beitr. Landesk. Nat. Mitt.*, **48**, 77–96.

Kohn, A.J. (1985) Gastropod paleoecology. *Stud. Geol.*, **13**, 174–189.

Król, J.J., **Jakubowicz, M.**, **Zapalski, M.K.** and **Berkowski, B.** (2018) Massive tabulates in competition for space: A case study from Aferdou el Mrakib (Middle Devonian, anti-atlas, Morocco). *Palaeogeogr. Palaeoclimatol. Palaeoecol.*, **497**, 105–116.

Król, J., **Denayer, J.**, **Wolniewicz, P.** and **Zapalski, M.** (2021) Heliolitid corals and their competitors: a case study from the Wellin patch reefs, Middle Devonian, Belgium. *Lethaia*, **54**, 540–557.

Lamarck, J.-B.P.A. (1801) *Système des animaux sans vertèbres, ou, Tableau général des classes, des ordres et des genres de ces animaux*. L'Auteur, Paris, 432 pp.

Langenstrassen, F. (1982) Sedimentologische und biofazielle Untersuchungen an Proben aus der Bohrung, Schwarzbachtal 1 (Rheinisches Schiefergebirge, Velberter Sattel). *Senckenb. Lethaea*, **63**, 315–333.

Langenstrassen, F. (1983) Neritic sedimentation of the lower and Middle Devonian in the Reinische Schiefergebirge east of the river Rhine. In: *Intracontinental Fold Belts, Case Studies in the Variscan Belt of Europe and the Damara Belt in Namibia* (Eds Martin, H. and Eder, F.W.), pp. 43–76. Springer-Verlag, Berlin, Heidelberg; New York, NY; Tokyo.

Lecompte, M. (1959) Certain data on the genesis and ecologic character of Frasnian reefs of the Ardennes. *Int. Geol. Rev.*, **1**, 1–23.

Leighton, L.R. (2000) Environmental distribution of spinose brachiopods from the Devonian of New York: test of the soft-subtrate hypothesis. *Palaios*, **15**, 184–193.

Lipps, J.H. and **Stanley, G.D., Jr.** (2016) Reefs through time: an evolutionary view. In: *Coral Reefs at the Crossroads* (Eds Hubbard, D.K., Rogers, C.S., Lipps, J.H. and Stanley, G.D., Jr.), pp. 175–196. Springer Nature, Dordrecht.

Lokier, S.W., **Wilson, M.E.J.** and **Burton, L.M.** (2009) Marine biota response to clastic sediment influx: a quantitative approach. *Palaeogeogr. Palaeoclimatol. Palaeoecol.*, **281**, 25–42.

Machel, H.G. and **Hunter, I.G.** (1994) Facies model for middle to late Devonian shallow-marine carbonates, with comparison to modern reefs: a guide for facies analysis. *Facies*, **30**, 155–176.

May, A. (1986) Biostratigraphische Untersuchungen im Mittel-Devon des Nordwest-Sauerlandes (Rheinisches Schiefergebirge). *Dortmunder Beitr. Landesk. Nat. Mitt.*, **20**, 23–55.

May, A. (1991) Die Fossilführung des westsauerländischen Givetiums (Devon; Rheinisches Schiefergebirge) in der Sammlung des Städtischen Museums Menden. *Geol. Pal. Westfalen*, **17**, 7–42.

May, A. (1999) Kommensalische *Syringopora*-Arten (Anthozoa; Tabulata) aus dem Devon von Zentral-Böhmen. *Münst. Forsch. Geol. Pal.*, **86**, 135–146.

May, A. and **Marks, S.** (2013) Eine Korallen-Fauna aus der Oberhonsel-Formation (Givetium; Devon) von Garbeck (West-Sauerland). *Dortmunder Beitr. Landesk. Nat. Mitt.*, **45**, 69–80.

Menning, M. and **Hendrich, A.** (2016) *Stratigraphische Tabelle von Deutschland 2016*. Deutsche Stratigraphische Kommission, Potsdam.

Meschede, M. (2018) *Geologie Deutschlands - Ein prozessorientierter Ansatz, 2. Auflage*. Springer, Berlin, Heidelberg, 252 pp.

Messing, C.G., **Meyer, D.L.**, **Siebeck, U.E.**, **Jermiin, L.S.**, **Vaney, D.I.** and **Rouse, G.W.** (2006) A modern soft-bottom, shallow water crinoid fauna (Echinodermata) from the great barrier reef, Australia. *Coral Reefs*, **25**, 164–168.

Mount, J.F. (1984) Mixing of siliciclastic and carbonate sediments in shallow shelf environments. *Geology*, **12**, 432–435.

Nichols, G. (2009) *Sedimentology and Stratigraphy*. Wiley-Blackwell, West Sussex, 419 pp.
Ricardo, G.F., **Jones, R.J.**, **Clode, P.L.**, **Humanes, A.** and **Negri, A.P.** (2015) Suspended sediments limit coral sperm availability. *Sci. Rep.*, **5**, 1–12.
Riegl, B.M. and **Piller, W.E.** (1999) Coral frameworks revisited – reefs and coral carpets in the northern Red Sea. *Coral Reefs*, **18**, 241–253.
Rogers, C.S. (1990) Responses of coral reefs and reef organisms to sedimentation. *Mar. Ecol. Prog. Ser.*, **62**, 185–202.
Rudwick, M.J.S. (1965) Ecology and paleoecology. In: *Treatise on Invertebrate Paleontology, Part H: Brachiopoda* (Ed. Moore, R.C.), pp. H199–H214. The Geological Society of America and the University of Kansas Press, Lawrence, KS.
Santodomingo, N., **Renema, W.** and **Johnson, K.G.** (2016) Understanding the murky history of the coral triangle: Miocene corals and reef habitats in East Kalimantan (Indonesia). *Coral Reefs*, **35**, 765–781.
Schulz, E. (1883) Die Eifelkalkmulde von Hillesheim. Nebst einem paläontolgischen Anhang. *Jb. Königl. Pr. Geol. Land. Bergakad. Berlin*, **1882**, 158–251.
Scrutton, C.T. (1998) The Palaeozoic corals, II: structure, variation and palaeoecology. *Proc. Yorks. Geol. Soc.*, **52**, 1–55.
Soja, C.M., **Gobetz, K.E.**, **Thibeau, J.**, **Zavala, E.** and **White, B.** (1996) Taphonomy and paleobiology implications of Middle Devonian (Eifelian) nautiloid concentrates, Alaska. *Palaios*, **11**, 422–436.
Stafford-Smith, M.G. (1993) Sediment-rejection efficiency of 22 species of Australian scleractinian corals. *Mar. Bio.*, **115**, 229–243.
Stafford-Smith, M.G. and **Ormond, R.F.G.** (1992) Sediment-rejection mechanisms of 42 species of Australian Scleractinian corals. *Aust. J. Mar. Freshwat. Res.*, **43**, 683–705.
Stainbrook, A. (1951) Substitution for the preoccupied brachiopod name *Hystricina*. *J. Washington Acad. Sci.*, **41**, 196.
Steininger, J. (1831) *Bemerkungen über die Versteinerungen, welche in dem Uebergangs-Kalkgebirge der Eifel gefunden werden*. Blattau'sche Buchdruckerei, Trier, 44 pp.
Struve, W. (1992) Neues zur Stratigraphie und Fauna des rhenotypen Mittel-Devon. *Senckenb. Lethaea*, **71**, 503–624.
Terry, R.D. and **Chilingar, G.V.** (1955) Summary of "Concerning some additional aids in studying sedimentary formations" by M. S. Shvetsov. *J. Sed. Petrol.*, **25**, 229–234.
Torsvik, T.H. and **Cocks, L.R.M.** (2017) *Earth History and Palaeogeography*. Cambridge University Press, Cambridge, 317 pp.
Trensch, J. and **Strasser, A.** (2011) Allogenic and autogenic process combined in the formation of shallow-water carbonate sequences (middle Berriasian, swiss and French Jura Mountains). *Swiss J. Geosci.*, **104**, 299–322.
Tucker, M.E. (2003) Mixed clastic-carbonate cycles and sequences: Quternary of Egypt and carboniferous of England. *Geol. Croatica*, **56**, 19–37.
Vinn, O. (2016) Symbiotic endobionts in Paleozoic stromatoporoids. *Palaeogeogr. Palaeoclimatol. Palaeoecol.*, **453**, 146–153.
Walker, K.R. and **Alberstadt, L.P.** (1975) Ecological succession as an aspect of structure in fossil communities. *Paleobiology*, **1**, 238–257.
Watkins, R. (2000) Silurian reef-dwelling brachiopods and their ecologic implications. *Palaios*, **15**, 112–119.
Watts, N.R. (1988) Carbonate particulate sedimentation and facies within the lower Silurian Högklint patch reefs of Gotland, Sweden. *Sed. Geol.*, **59**, 93–113.
Watts, N.R. and **Riding, R.** (2000) Growth of rigid high-relief patch reefs, mid-Silurian, Gotland, Sweden. *Sedimentology*, **47**, 979–994.
Wilson, M.E.J. and **Lokier, S.W.** (2002) Siliciclastic and volcaniclastic influences on equatorial carbonates: insights from the Neogene of Indonesia. *Sedimentology*, **49**, 583–601.
Wolanski, E., **Fibricius, K.**, **Spagnol, S.** and **Brinkman, R.** (2005) Fine sediment budget on an inner-shelf coral-fringed Island, great barrier reef of Australia. *Estuar. Coast. Shelf Sci.*, **65**, 153–158.
Wood, R. (1998) The ecological evolution of reefs. *Ann. Rev. Ecol. System.*, **29**, 179–206.
Wood, R. (1999) *Reef Evolution*. Oxford University Press, New York, NY, 414 pp.
Wood, R. (2000) Palaeoecology of a late Devonian back reef: Canning Basin, Western Australia. *Palaeontology*, **43**, 671–703.
Woolfe, K.J. and **Larcombe, P.** (1999) Terrigenous sedimentation and coral reef growth: a conceptual framework. *Mar. Geol.*, **155**, 331–345.
Zapalski, M.K., **Baird, A.H.**, **Bridge, T.** and **Jakubowicz, M.** (2021) Unusual shallow water Devonian coral community from Queensland and its recent analogues from the inshore great barrier reef. *Coral Reefs*, **40**, 417–431.
Zatoń, M., **Borszcz, T.**, **Berkowski, B.**, **Rakociński, M.**, **Zapalski, M.K.** and **Zhuravlev, A.V.** (2015) Paleoecology and sedimentary environment of the late Devonian coral biostrome from the central Devonian field, Russia. *Palaeogeogr. Palaeoclimatol. Palaeoecol.*, **424**, 61–75.
Zecchin, M. and **Catuneanu, O.** (2017) High-resolution sequence stratigraphy of clastic shelves VI: mixed siliciclastic-carbonate systems. *Mar. Petrol. Geol.*, **88**, 712–723.
Zweifler, A., **O'Leary, M.**, **Morgan, K.** and **Browne, N.** (2021) Turbid coral reefs: past, present and future – a review. *Diversity*, **13**, 251.

Manuscript received 15 August 2022; revision accepted 10 January 2023

Supporting Information

Additional information may be found in the online version of this article:

Table S1. Results of the X-ray diffraction method in wt.-%.

Table S2. Distribution of the different bioconstructors within the Klutert biostrome and the overlying Brachiopod Coquina.

Table S3. Values of the clastic matrix content based on acid digestion.

